SIAM J. SCI. COMPUT.
Vol. 33, No. 1, pp. 223–249

TIME-INTEGRATION SCHEMES FOR THE FINITE ELEMENT DYNAMIC SIGNORINI PROBLEM*

DAVID DOYEN†, ALEXANDRE ERN‡, AND SERGE PIPERNO‡

Abstract. A large variety of discretizations have been proposed in the literature for the numerical solution of the dynamic Signorini problem. We classify the different discretizations into four groups. The first three groups correspond to different ways of enforcing the contact condition: exact enforcement, enforcement with penalty, and enforcement with contact condition in velocity. The fourth approach is based on a modification of the mass matrix. Numerical simulations on two one-dimensional benchmark problems with analytical solutions illustrate the properties of representative methods within each class, focusing first on spurious oscillations triggered by contact and then on energy behavior after multiple impacts. Selected schemes are also tested on a two-dimensional benchmark.

Key words. elastodynamics, frictionless unilateral contact, time-integration schemes, finite elements, modified mass method

AMS subject classifications. 65M20, 65M60, 74H15, 74M15, 74S05

DOI. 10.1137/100791440

1. Introduction.

The design of robust and efficient numerical methods for dynamic contact problems has motivated a large amount of work over the last two decades and remains challenging. Here, we focus on the dynamic Signorini problem, which models the infinitesimal deformations of a solid body that can come into contact with a rigid obstacle. This problem is the simplest dynamic contact problem, but also the first step toward more complex situations such as multibody problems, large deformation problems, contact with friction, etc. For an overview of the different contact problems, we refer the reader to [21, 25, 38].

In structural dynamics, the usual space-time discretization combines finite elements in space and a time-stepping scheme. In this framework, the discretization of the dynamic Signorini problem involves mainly three choices: (i) the finite element space, (ii) the enforcement of the contact condition, (iii) the time-stepping scheme. The combination of these three ingredients presents some difficulties. For instance, it is well known that the combination of an exact enforcement of the contact condition and an implicit Newmark scheme yields spurious oscillations as well as poor energy behavior, that is, sizeable deviations from the exact value. Moreover, the combination of an exact enforcement and an explicit scheme is not straightforward, whereas the use of a penalty contact condition tightens the stability condition of explicit schemes. Consequently, various alternative discretizations have been designed for the dynamic Signorini problem. The aim of this work is to classify the different discretizations and to numerically illustrate their main properties.

We classify the discretizations into four groups. The first three groups correspond to different ways of enforcing the contact condition: exact enforcement [6, 8, 18, 27,

*Submitted to the journal's Computational Methods in Science and Engineering section April 7, 2010; accepted for publication (in revised form) November 2, 2010; published electronically February 3, 2011.
http://www.siam.org/journals/sisc/33-1/79144.html
†Electricité de France (EDF R&D), 1 avenue du Général de Gaulle, 92141 Clamart Cedex, France (david.doyen@edf.fr).
‡Université Paris-Est, CERMICS, Ecole des Ponts, 77455 Marne la Vallée Cedex 2, France (ern@cermics.enpc.fr, serge.piperno@enpc.fr).

31, 32, 36, 37], enforcement with penalty [1, 3, 15], and enforcement with contact condition in velocity [2, 3, 26]. The fourth approach is based on a modification of the mass matrix [14, 20]; it can be seen as an alternative choice of the finite element space. These four classes yield different space semidiscrete problems, which in turn can be discretized in time using various time-stepping schemes, either implicit or semiexplicit. We select representative discretizations within each class and examine their main properties: presence of spurious oscillations, energy behavior after multiple impacts, and stability in the case of explicit schemes. By energy conservation we mean that the variation of the energy is equal to the work of the external forces (the contact forces should not work). To illustrate these properties, numerical simulations on two one-dimensional (1D) benchmarks have been performed. The first benchmark, the impact of an elastic bar on a rigid surface, is well known and allows one to detect spurious oscillations. The second, for which we derive the exact solution, deals with the bounces of an elastic bar and is geared toward energy behavior, insofar as multiple impacts occur; it is, to our knowledge, a new benchmark. Additionally, some of the schemes are tested on a two-dimensional (2D) benchmark (without analytical solution) associated with the impact and multiple bounces of a disk on a rigid surface. Some of the presented Newmark-based schemes are also compared in three dimensions in [23]. The mathematical analysis of the different methods is beyond the scope of this article, but we mention, whenever they exist, the theoretical results (well-posedness of the discrete problems and convergence of the discrete solutions). Dynamic contact problems yield shock waves, and spurious oscillations appear near the shock in the numerical solutions, owing to the so-called Gibbs phenomenon (see, e.g., [13] and references therein). These oscillations can be eliminated using dissipative schemes (or, equivalently, by filtering). This issue, being important but not specific to dynamic contact problems, is not further addressed here (see also Remark 4.4).

The material is organized as follows. We formulate the dynamic Signorini problem in the continuous setting (section 2.1), and we introduce the main ingredients for its approximation (sections 2.2 and 2.3). We present the two 1D benchmark problems with their analytical solutions (section 3). We describe the four classes of discretizations together with numerical results in one dimension: exact enforcement of the contact condition (section 4), enforcement with penalty contact condition (section 5), enforcement with contact condition in velocity (section 6), and modification of the mass matrix (section 7). Finally, we present numerical results on the 2D benchmark for selected schemes (section 8) and draw some conclusions (section 9).

2. The dynamic Signorini problem.

2.1. Governing equations. We consider the infinitesimal deformations of a body occupying a reference domain $\Omega \subset \mathbb{R}^d$ ($d \in \{1, 2, 3\}$) during a time interval $[0, T]$. The tensor of elasticity is denoted by $\mathcal{A}$, and the mass density is denoted by ρ. An external load f is applied to the body. Let $u : (0,T)\times\Omega \to \mathbb{R}^d$, $\epsilon(u) : (0,T)\times\Omega \to \mathbb{R}^{d,d}$, and $\sigma(u) : (0,T) \times \Omega \to \mathbb{R}^{d,d}$ be the displacement field, the linearized strain tensor, and the stress tensor, respectively. Denoting time-derivatives by dots, the momentum conservation equation reads

$$\rho\ddot{u} - \operatorname{div}\sigma = f, \quad \sigma = \mathcal{A} : \epsilon, \quad \epsilon = \frac{1}{2}(\nabla u + {}^{\mathrm{T}}\nabla u) \quad \text{in } \Omega \times (0,T). \tag{2.1}$$

The boundary $\partial\Omega$ is partitioned into three disjoint open subsets, Γ^D, Γ^N, and Γ^c. Dirichlet and Neumann conditions are prescribed on Γ^D and Γ^N, respectively $u = u_D$ on $\Gamma^D \times (0,T)$ and $\sigma \cdot n = f_N$ on $\Gamma^N \times (0,T)$, where n denotes the outward unit

normal to Ω. We set $u_n := u_{|\partial\Omega} \cdot n$ and $\sigma_n := n \cdot \sigma_{|\partial\Omega} \cdot n$, the normal displacement and the normal stress on $\partial\Omega$, respectively. On Γ^c, a unilateral contact condition, also called Signorini condition, is imposed:

$$u_n \leq 0,\ \sigma_n(u) \leq 0,\ \sigma_n(u)u_n = 0 \quad \text{on } \Gamma^c \times (0,T). \tag{2.2}$$

At the initial time, the displacement and velocity fields are prescribed. The above problem is an evolution partial differential equation under unilateral constraints. Here, the equation is second-order in time, and the constraint holds on the displacement; this is not the most favorable case. The existence and uniqueness of a solution has been proven only in one dimension, when the contact boundary is reduced to a point [28, 11]. In one dimension, it has also been proven that the variation of energy is equal to the work of the external forces; the contact force does not work [28, 11]. In higher dimensions, the existence of a solution is proven in the case of a viscoelastic material, and, under certain assumptions, existence and uniqueness are proven for the wave equation [28, 11].

2.2. Basic time-integration schemes in linear elastodynamics. In this section, we briefly recall some basic facts about time-integration schemes in linear elastodynamics; most of this material can be found in [17]. First, we discretize the problem in space with a finite element method. To simplify the notation, we still denote by u the space semidiscrete displacement. The number of degrees of freedom is denoted by N_d. Let K, M, and $F(t)$ be the stiffness matrix, the mass matrix, and the column vector of the external forces, respectively. The space semidiscrete problem consists of seeking $u : [0,T] \to \mathbb{R}^{N_d}$ such that, for all $t \in [0,T]$,

$$M\ddot{u}(t) + Ku(t) = F(t), \tag{2.3}$$

with the initial conditions $u(0) = u^0$ and $\dot{u}(0) = v^0$. For solving such a system of ordinary differential equations (ODEs), linear one-step schemes are the most frequently used. For simplicity, the interval $[0,T]$ is divided into equal subintervals of length Δt. We set $t^n = n\Delta t$ and denote by u^n, $\dot{u}^n$, and $\ddot{u}^n$ the approximations of $u(t^n)$, $\dot{u}(t^n)$, and $\ddot{u}(t^n)$, respectively. We define the convex combination $\square^{n+\omega} := (1-\omega)\square^n + \omega\square^{n+1}$, where $\square$ stands for u, $\dot{u}$, $\ddot{u}$ or t, and $\omega \in [0,1]$. We use a slightly different definition for the external load, namely, $F^{n+\alpha} := F(t^{n+\alpha})$; for instance, $F^{n+\frac{1}{2}} = F(t^{n+\frac{1}{2}})$ generally differs from $\frac{1}{2}(F^n + F^{n+1})$. Moreover, at time t^n, the energy of the system is given by $\mathcal{E}^n := \frac{1}{2}{}^{\mathrm{T}}\dot{u}^n M\dot{u}^n + \frac{1}{2}{}^{\mathrm{T}}u^n K u^n$. Now we can formulate some of the most common time-stepping schemes in linear elastodynamics.

DISCRETIZATION 2.1 (Hilber–Hughes–Taylor (HHT)-Newmark). *Seek* $u^{n+1}, \dot{u}^{n+1}, \ddot{u}^{n+1} \in \mathbb{R}^{N_d}$ *such that*

$$M\ddot{u}^{n+1} + Ku^{n+1+\alpha} = F^{n+1+\alpha}, \tag{2.4}$$

$$u^{n+1} = u^n + \Delta t\ \dot{u}^n + \frac{\Delta t^2}{2}\ \ddot{u}^{n+2\beta}, \tag{2.5}$$

$$\dot{u}^{n+1} = \dot{u}^n + \Delta t\ \ddot{u}^{n+\gamma}, \tag{2.6}$$

where α, β, γ *are real parameters. The choice* $\alpha = 0$ *yields Newmark schemes, while the choice* $\alpha \in [-1/3, 0]$, $\beta = 1/4(1-\alpha)^2$, *and* $\gamma = 1/2 - \alpha$ *yields HHT schemes.*

DISCRETIZATION 2.2 (midpoint). *Seek* $u^{n+1},\ \dot{u}^{n+1},\ \ddot{u}^{n+\frac{1}{2}} \in \mathbb{R}^{N_d}$ *such that*

$$M\ddot{u}^{n+\frac{1}{2}} + Ku^{n+\frac{1}{2}} = F^{n+\frac{1}{2}}, \tag{2.7}$$

$$u^{n+1} = u^n + \Delta t\ \dot{u}^{n+\frac{1}{2}}, \tag{2.8}$$

$$\dot{u}^{n+1} = \dot{u}^n + \Delta t\ \ddot{u}^{n+\frac{1}{2}}. \tag{2.9}$$

DISCRETIZATION 2.3 (central differences). *Seek* $u^{n+1} \in \mathbb{R}^{N_d}$ *such that*

$$M\left(\frac{u^{n+1} - 2u^n + u^{n-1}}{\Delta t^2}\right) + Ku^n = F^n. \tag{2.10}$$

HHT schemes are implicit, unconditionally stable, second-order accurate, and dissipative in the high frequencies. The amount of dissipation is controlled by the parameter α. Newmark schemes do not, in general, conserve the energy; such schemes instead conserve the quadratic form $\mathcal{E}^n_{\beta,\gamma} := \mathcal{E}^n + \frac{\Delta t^2}{2}\left(\beta - \frac{1}{2}\gamma\right)^{\mathrm{T}}\ddot{u}^n M\ddot{u}^n$ since there holds [24]

$$\begin{aligned}\mathcal{E}^{n+1}_{\beta,\gamma} - \mathcal{E}^n_{\beta,\gamma} = {}^{\mathrm{T}}&\left(\frac{1}{2}(F^{n+1} + F^n) + \left(\gamma - \frac{1}{2}\right)(F^{n+1} - F^n)\right)(u^{n+1} - u^n)\\ &- \left(\gamma - \frac{1}{2}\right)\left({}^{\mathrm{T}}(u^{n+1} - u^n)K(u^{n+1} - u^n)\right.\\ &\qquad\left. + \left(\beta - \frac{1}{2}\gamma\right)^{\mathrm{T}}(\ddot{u}^{n+1} - \ddot{u}^n)M(\ddot{u}^{n+1} - \ddot{u}^n)\right).\end{aligned}$$

The quadratic form $\mathcal{E}^n_{\beta,\gamma}$ coincides with the energy only if $\beta = \frac{1}{2}\gamma$. For $\beta \neq \frac{1}{2}\gamma$, we refer to $\mathcal{E}^n_{\beta,\gamma}$ as a shifted energy; the sign of the difference between $\mathcal{E}^n_{\beta,\gamma}$ and $\mathcal{E}^n$ depends only on the sign of $(\beta - \frac{1}{2}\gamma)$. The particular choice $\beta = 1/4$, $\gamma = 1/2$ yields an implicit, unconditionally stable, and second-order accurate scheme. It is energy-conserving in the sense that

$$\mathcal{E}^{n+1} - \mathcal{E}^n = {}^{\mathrm{T}}\left(\frac{F^{n+1} + F^n}{2}\right)(u^{n+1} - u^n).$$

The midpoint scheme is implicit, unconditionally stable, and second-order accurate. It is energy-conserving in the sense that

$$\mathcal{E}^{n+1} - \mathcal{E}^n = {}^{\mathrm{T}}F^{n+\frac{1}{2}}(u^{n+1} - u^n).$$

The central difference scheme is explicit (lumping the mass matrix avoids solving any linear system), conditionally stable, and second-order accurate. Here it is written as a two-step linear scheme involving only the displacement, but it can be formulated as a one-step scheme. Actually, it is a Newmark scheme with parameters $\beta = 0$, $\gamma = 1/2$; the velocity and acceleration are then $\dot{u}^n = \frac{1}{2\Delta t}(u^{n+1} - u^{n-1})$ and $\ddot{u}^n = \frac{1}{\Delta t^2}(u^{n+1} - 2u^n + u^{n-1})$. The central difference scheme does not conserve the energy $\mathcal{E}^n$ but the shifted energy $\mathcal{E}^n_{0,\frac{1}{2}}$ in the sense that

$$\mathcal{E}^{n+1}_{0,\frac{1}{2}} - \mathcal{E}^n_{0,\frac{1}{2}} = {}^{\mathrm{T}}\left(\frac{F^{n+1} + F^n}{2}\right)(u^{n+1} - u^n).$$

There exist also explicit schemes with high-frequency dissipation, such as the Chung–Hulbert or Tchamwa–Wielgosz schemes (see [30] and references therein).

2.3. Enforcing the contact condition. The enforcement of a contact condition in a finite element setting has been widely studied in the case of the static Signorini problem [21]. We assume that the mesh is compatible with the partition of the boundary. Let N_c be the number of nodes lying on the contact boundary. We define the linear normal trace operator on Γ^c, $g : v \longmapsto -v_{|\Gamma} \cdot n$, and the associated matrix G. Note that the dimension of G is $N_c \times N_d$. We denote by $\{G_i\}_{1 \le i \le N_c}$ the rows of the matrix G. Thus, $G_i u$ yields the value of the normal displacement at the ith node of the contact boundary. With an exact enforcement, the static Signorini problem consists of seeking a displacement $u \in \mathbb{R}^{N_d}$ and a contact pressure $r \in \mathbb{R}^{N_c}$ such that

$$Ku = F + {}^{\mathrm{T}}Gr, \tag{2.11}$$

$$Gu \ge 0, \quad r \ge 0, \quad {}^{\mathrm{T}}rGu = 0. \tag{2.12}$$

Here the problem is formulated as a complementarity problem. Other formalisms can be found in the literature, e.g., variational inequality, Lagrangian formulation, and formulation with subderivatives. If the matrix K is positive definite, problem (2.11)–(2.12) has a unique solution. For solving this problem, a large variety of methods have been developed [21, 38]: Uzawa algorithms, active set methods, semismooth Newton methods, the Lemke algorithm, the monotone multigrid method, etc.

Penalty formulations are another classical way of dealing with constrained problems. We have to define a penalty function $R_\epsilon : \mathbb{R}^{N_c} \to \mathbb{R}^{N_c}$. For instance, we can choose $R_\epsilon(v) = \frac{1}{\epsilon}(v)^-$, where $(v)^-$ denotes the negative part of v. The penalized static Signorini problem consists now of seeking $u \in \mathbb{R}^{N_d}$ such that

$$Ku = F + {}^{\mathrm{T}}GR_\epsilon(Gu). \tag{2.13}$$

A third way of enforcing the contact condition, specific to the dynamic problem, is to replace the Signorini condition by an approximation involving the velocity instead of the displacement [11, 29]. Assume that $u_n = 0$ at a certain time t^c. Then, on a short time interval afterwards, $u_n \approx (t - t^c)\dot{u}_n$. This motivates the following contact condition in velocity:

$$\dot{u}_n \le 0, \ \sigma_n(u) \le 0, \ \sigma_n(u)\dot{u}_n = 0 \quad \text{on } \Gamma^c. \tag{2.14}$$

It must be stressed that condition (2.14) is applicable only during contact phases. This condition is not applicable during noncontact phases because a positive normal velocity is not allowed.

3. 1D benchmark problems. To compare the different methods, we test them on two 1D problems. Both problems can be formulated in the same setting. We consider an elastic bar dropped against a rigid ground. The bar is dropped, undeformed, from a height h_0, with an initial velocity $-v_0$, under a gravity acceleration $g_0 \ge 0$. The length of the bar is denoted by L, the Young modulus by E, and the density by ρ. Let $c_0 := \sqrt{\frac{E}{\rho}}$ denote the wave speed. The reference domain is $\Omega = [0, L]$. In this context, the governing equations presented in section 2.1 for the continuous problem take the form

$$\rho\ddot{u} - E\frac{\partial^2 u}{\partial x^2} = -\rho g_0 \quad \text{in } \Omega \times (0, T), \tag{3.1}$$

$$u(0, t) \ge 0, \ r(t) \ge 0, \ r(t)u(0, t) = 0 \quad \text{on } (0, T), \tag{3.2}$$

$$\frac{\partial u}{\partial x}(L, t) = 0 \quad \text{on } (0, T), \quad u(\cdot, 0) = h_0, \quad \dot{u}(\cdot, 0) = -v_0, \tag{3.3}$$

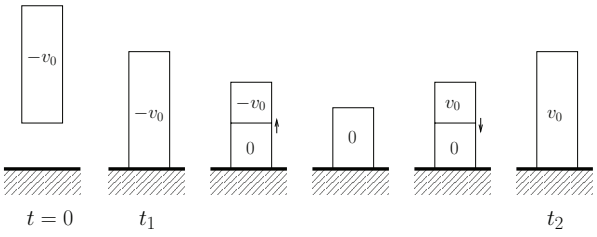

FIG. 1. *Impact of an elastic bar.*

where u is the scalar-valued displacement of the bar and r the contact pressure equal to the normal stress $-E\frac{\partial u}{\partial x}$ at $x=0$. Problem (3.1)–(3.3) has a unique solution, and the variation of the energy is equal to the work of the gravity force [28],

$$\frac{d}{dt}\left(\frac{1}{2}\int_\Omega \rho\dot{u}^2+\frac{1}{2}\int_\Omega E\left|\frac{\partial u}{\partial x}\right|^2\right)=\int_\Omega -\rho g_0\dot{u}\quad\forall t\in[0,T]. \tag{3.4}$$

In the first problem, $v_0>0$ and $g_0=0$ so that there is a single impact. This benchmark has been widely used in the literature (see, e.g., [38]). It enables us to examine the possible spurious oscillations triggered by the numerical schemes. In the second problem, $v_0=0$ and $g_0>0$, so that the bar can make several bounces. With a suitable choice of parameters, the motion of the bar is periodic in time, and we can calculate the exact solution. This benchmark enables us to examine the time evolution of energy after multiple impacts and is, to our knowledge, new.

3.1. Impact of an elastic bar. Let us describe the solution of the first problem (Figure 1). Before the impact, the bar is undeformed and has a uniform velocity $-v_0$. The bar reaches the ground at time $t_1:=\frac{h_0}{v_0}$. After the impact, the bar stays in contact with the ground. A shock wave travels from the bottom of the bar to the top. Above the shock wave, the velocity is $-v_0$; below, the velocity is zero. Then, the shock wave travels from the top to the bottom. Above the shock wave, the velocity is v_0; below, the velocity is still zero. As soon as the wave reaches the bottom, the bar takes off, undeformed, with a uniform velocity v_0. The speed of the shock wave is c_0. Thus, the wave takes a time $\tau_w:=\frac{L}{c_0}$ to travel along the bar, and the bar takes off at time $t_2:=t_1+2\tau_w$. The analytical solution can be easily expressed using travelling wave solutions. Defining the auxiliary function $H_v(x,t)=-v\min(x/c_0,\tau_w-|t-\tau_w|)$, the exact solution is

$$u(x,t)=\begin{cases}h_0-v_0t & \text{if } t\le t_1,\\ H_{v_0}(x,t-t_1) & \text{if } t_1<t\le t_2,\\ v_0(t-t_2) & \text{if } t_2<t.\end{cases}$$

In particular, the displacement at the bottom of the bar and the contact pressure are

$$u(0,t)=\begin{cases}h_0-v_0t & \text{if } t\le t_1,\\ 0 & \text{if } t_1<t\le t_2,\\ v_0(t-t_2) & \text{if } t_2<t,\end{cases}\qquad r(t)=\begin{cases}0 & \text{if } t\le t_1,\\ \frac{Ev_0}{c_0} & \text{if } t_1<t\le t_2,\\ 0 & \text{if } t_2<t.\end{cases}$$

These two quantities are represented in Figure 2 (with the parameters chosen in section 3.3).

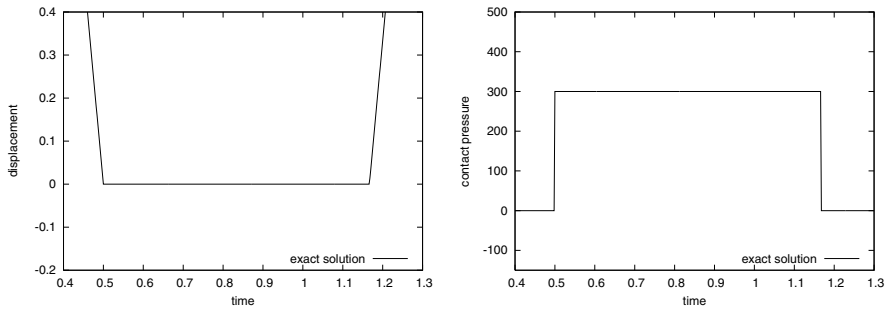

FIG. 2. *Impact of an elastic bar. Displacement at the bottom of the bar (left) and contact pressure (right).*

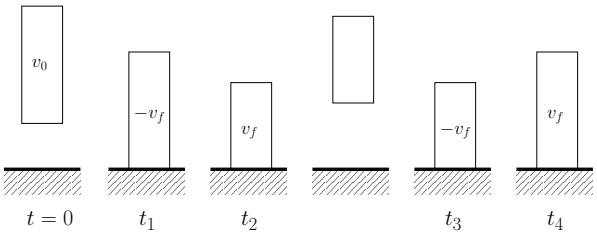

FIG. 3. *Bounces of an elastic bar.*

3.2. Bounces of an elastic bar. In the second problem (Figure 3), the bar is dropped, undeformed, with a zero initial velocity. It takes a time $\tau_f := \sqrt{\frac{2h_0}{g_0}}$ to reach the ground. At the impact, at time $t_1 := \tau_f$, the bar is undeformed and has uniform velocity $-v_f$, where $v_f := \sqrt{2h_0g_0}$. After the impact, as in the previous benchmark, the bar stays in contact with the ground during a time $2\tau_w$. During this contact phase, the response of the bar is the superposition of a shock wave due to velocity at the impact and a vibration due to the gravity, as reflected by the series S_1 and S_2 below. When the bar takes off, at time $t_2 := t_1 + 2\tau_w$, it has a uniform velocity v_f but it is compressed. (By symmetry, $u(x, t_2) = \tilde{u}(x) := \frac{g_0}{c_0^2}(x^2 - 2Lx)$ is twice the static deformation with homogeneous Dirichlet and Neumann conditions at $x = 0$ and $x = L$, respectively.) Consequently, during the flight phase, the response of the bar is the superposition of a rigid parabolic motion (due to the gravity and the velocity) and a vibration (due to the initial deformation). If we choose $\tau_f = p\tau_w$ for a positive integer p (for instance, $\tau_f = 3\tau_w$), we can ensure that the bar reaches the ground with uniform velocity $-v_f$ and with displacement field $\tilde{u}$. When we do this, the second impact occurs at time $t_3 := t_2 + 2\tau_f = t_2 + 6\tau_w$. When the bar takes off again, at time $t_4 := t_3 + 2\tau_w$, it is undeformed and has a uniform velocity v_f. The next flight phase is a rigid parabolic movement. Then this sequence of two contact phases and two flight phases repeats periodically. To compute the analytical solution, we use a decomposition on the eigenmodes in addition to the travelling wave solutions. We set $t_{4k+1} = 3\tau_w + 16k\tau_w$, $t_{4k+2} = t_{4k+1} + 2\tau_w$, $t_{4k+3} = t_{4k+1} + 8\tau_w$, and $t_{4k+4} = t_{4k+1} + 10\tau_w$. We also define the auxiliary functions $P(x,t) = h_0 - \frac{1}{2}g_0(t - \tau_f)^2$, $S_1(x,t) = \sum_{n=1}^{\infty} a_n(1 - \cos(c_0\nu_n t))\sin(\nu_n x)$, $S_2(x,t) = -\frac{2g_0L^2}{3c_0^2} + \sum_{n=1}^{\infty} b_n \cos(c_0\lambda_n t)\cos(\lambda_n x)$, where $a_n = \frac{-2g_0}{c_0^2 L\nu_n^3}$, $\nu_n = (n - \frac{1}{2})\frac{\pi}{L}$, $b_n = \frac{4g_0}{c_0^2\lambda_n^2}$,

$\lambda_n = n\frac{\pi}{L}$. The function S_1 corresponds to the vibration of a bar, clamped at its bottom, initially at rest, under a gravity g_0. The function S_2 corresponds to the vibration of a bar, free at its two extremities, with the initial displacement $\tilde{u}$, a zero initial velocity, and no external force. The computation of the series S_1 and S_2 is standard; see [7], for instance. The exact solution is

$$u(x,t) = \begin{cases} P(x, t+\tau_f) & \text{if } t \le t_1, \\ H_{v_f}(x, t - t_{4k+1}) + S_1(x, t - t_{4k+1}) & \text{if } t_{4k+1} < t \le t_{4k+2}, \\ P(x, t - t_{4k+2}) + S_2(x, t - t_{4k+2}) & \text{if } t_{4k+2} < t \le t_{4k+3}, \\ H_{v_f}(x, t_{4k+4} - t) + S_1(x, t_{4k+4} - t) & \text{if } t_{4k+3} < t \le t_{4k+4}, \\ P(x, t - t_{4k+4}) & \text{if } t_{4k+4} < t \le t_{4(k+1)+1}. \end{cases}$$

The displacement at the bottom of the bar is represented in Figure 4 (with the parameters chosen in section 3.3).

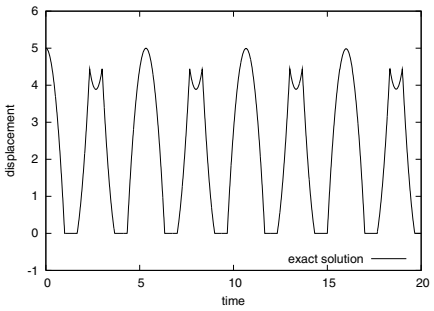

FIG. 4. *Bounces of an elastic bar. Displacement at the bottom of the bar.*

3.3. Numerical simulations. The parameters used in the numerical simulations are $E = 900$, $\rho = 1$, $L = 10$, $h_0 = 5$. In the first benchmark, $v_0 = 10$, $g_0 = 0$; in the second benchmark, $v_0 = 0$, $g_0 = 10$. The bar is discretized with a uniform mesh size Δx, and linear finite elements are used. We define $\nu_c := c_0 \frac{\Delta t}{\Delta x}$ as the Courant number, which is the relevant ratio to link the mesh size and the time step. In particular, central difference schemes with lumped mass matrix are stable in the linear case under the condition $\nu_c \le 1$. In what follows, we take $\nu_c = 1.5$ for unconditionally stable schemes and $\nu_c = 0.75$ (thereby halving the time step) for central difference schemes. To describe the numerical results, we consider the following quantities: the displacement at the bottom node of the bar (denoted by u_0^n), the stress at the bottom node of the bar (denoted by $(Ku^n)_0$), the contact pressure r^n, and the energy $\mathcal{E}^n - {}^{\mathrm{T}}Fu^n$ (the load vector being time-independent, we denote it by F). Note that, because of the finite element discretization, the stress at the bottom node and the contact pressure are not equal.

4. Discretizations with exact enforcement of the contact condition. In this section we combine standard finite elements in space and an exact enforcement of the contact condition at each node of the contact boundary. This leads to the semidiscrete problem

$$M\ddot{u}(t) + Ku(t) = F(t) + {}^{\mathrm{T}}Gr(t), \tag{4.1}$$

$$Gu(t) \ge 0, \quad r(t) \ge 0, \quad {}^{\mathrm{T}}r(t)Gu(t) = 0. \tag{4.2}$$

Problem (4.1)–(4.2) is a system of differential equations under unilateral constraints. The same kind of formulation arises in rigid-body dynamics with impact [5, 35], so the mathematical results and the numerical methods developed in this framework can in general be applied to problem (4.1)–(4.2). Mathematically, this problem turns out to be delicate. First, the functional framework is not obvious. Due to the unilateral constraints, the velocity can be discontinuous, and there is in general no strong solution (i.e., twice differentiable in time) to this problem. One possibility is to look for a weak solution such that the displacement u is continuous in time, the velocity $\dot{u}$ is a function with bounded variation in time, and the acceleration $\ddot{u}$ and the contact pressure r are measures (they contain impulses). Second, this weak solution is in general not unique. Consider the simple example of a point mass impacting a rigid foundation. Before the impact, the motion of the point mass is uniquely determined. After the impact, an infinity of velocities and trajectories are admissible. To recover uniqueness, an additional condition, specifying the velocity after an impact, is needed. Denoting by v^- the normal velocity before the impact and by v^+ the normal velocity after the impact, a usual approach is to prescribe $v^+ = -ev^-$, where e is a nonnegative parameter. In the present space semidiscrete setting, it seems reasonable to take $e = 0$. Indeed, in the dynamic Signorini problem, the unilateral constraint holds on the boundary, and the boundary does not bounce after an impact. We can now formulate the semidiscrete problem with impact law.

PROBLEM 4.1. *Seek a displacement* $u : [0,T] \to \mathbb{R}^{N_d}$ *and a contact pressure* $r : [0,T] \to \mathbb{R}^{N_c}$ *such that*

$$M\ddot{u} + Ku = F + {}^{\mathrm{T}}Gr, \tag{4.3}$$

$$Gu \geq 0, \quad r \geq 0, \quad {}^{\mathrm{T}}rGu = 0, \tag{4.4}$$

$${}^{\mathrm{T}}r_i(t)G_i\dot{u}(t^+) = 0 \quad \textit{if} \quad G_iu(t) = 0, \tag{4.5}$$

with the initial conditions $u(0) = u^0$ *and* $\dot{u}(0) = v^0$.

Equation (4.5) constitutes the impact law. Most of the mathematical terms in (4.3)–(4.5) must be understood in the sense of measures. In particular, ${}^{\mathrm{T}}rGu$ and ${}^{\mathrm{T}}r_i(t)G_i\dot{u}(t^+)$ should be defined with suitable duality products. For more details, we refer the reader to [5, 35].

Remark 4.1. The impact law (4.5) is a consequence of the discretization in space. Indeed, the continuous problem does not need an impact law to have a unique solution. This fact is proven in one dimension [11, 28]; in higher dimensions, uniqueness is still an open problem, but the difficulty does not seem to come from the absence of an impact law.

Remark 4.2. Another difference from the continuous solution is that the semidiscrete solution does not conserve the energy since there is a loss of energy at each impact of a node. Actually, energy is conserved for $e = 1$, but this is not satisfactory since the contact is never established for a time interval of nonzero length.

Remark 4.3. The impact law is different from the concept of persistency condition sometimes encountered in the literature [1, 25, 26, 27]. The persistency condition is defined in the continuous setting and in the fully discrete setting. It requires that the contact force does not work. Note that, in the continuous problem, the persistency condition seems to be a consequence of the Signorini condition (it is at least proven in one dimension).

4.1. Implicit schemes. We consider first dissipative schemes and then schemes dealing with the impact.

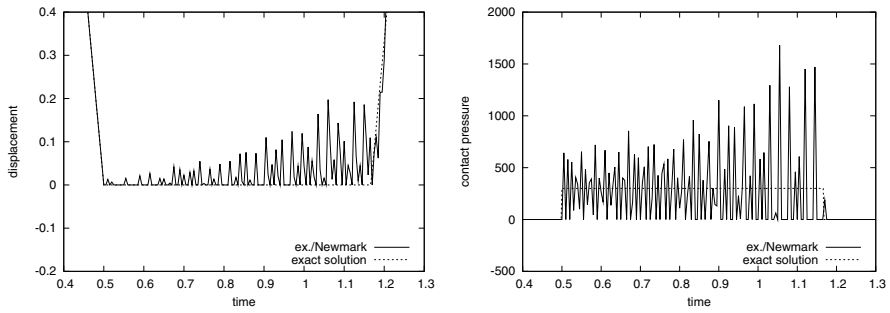

FIG. 5. *Impact of an elastic bar. Displacement u_0^n (left) and contact pressure r^n (right). Discretization* 4.1 *with $\alpha = 0$, $\beta = 1/4$, and $\gamma = 1/2$. $\Delta x = 0.1$, $\Delta t = 0.005$, $\nu_c = 1.5$.*

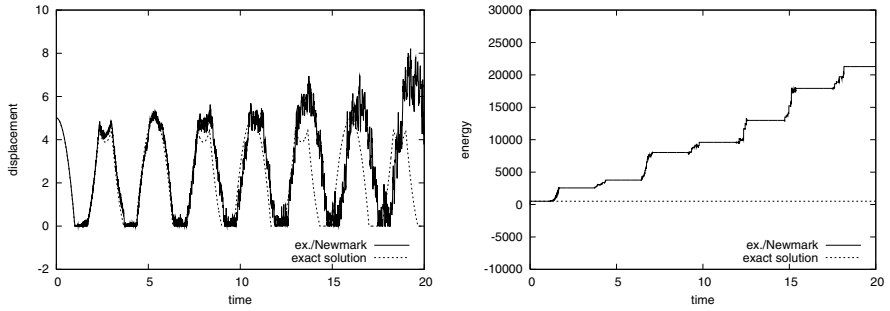

FIG. 6. *Bounces of an elastic bar. Displacement u_0^n (left) and energy $\mathcal{E}^n - {}^{\mathrm{T}}Fu^n$ (right). Discretization* 4.1 *with $\alpha = 0$, $\beta = 1/4$, and $\gamma = 1/2$. $\Delta x = 0.1$, $\Delta t = 0.005$, $\nu_c = 1.5$.*

4.1.1. Dissipative schemes. To motivate the discussion, let us begin with an ill-founded discretization. We choose a Newmark scheme (trapezoidal rule) for the elastodynamics part, and we enforce the contact condition (4.4) at a certain time, say t^{n+1}. We pay no attention to the impact law (4.5). This choice corresponds to Discretization 4.1 with $\alpha = 0$, $\beta = 1/4$, $\gamma = 1/2$.

DISCRETIZATION 4.1 (HHT-Newmark). *Seek u^{n+1}, $\dot{u}^{n+1}$, $\ddot{u}^{n+1} \in \mathbb{R}^{N_d}$, and $r^{n+1} \in \mathbb{R}^{N_c}$ such that*

$$M\ddot{u}^{n+1} + Ku^{n+1+\alpha} = F^{n+1+\alpha} + {}^{\mathrm{T}}Gr^{n+1}, \tag{4.6}$$

$$Gu^{n+1} \geq 0, \quad r^{n+1} \geq 0, \quad {}^{\mathrm{T}}r^{n+1}Gu^{n+1} = 0, \tag{4.7}$$

$$u^{n+1} = u^n + \Delta t\dot{u}^n + \frac{\Delta t^2}{2}\,\ddot{u}^{n+2\beta}, \tag{4.8}$$

$$\dot{u}^{n+1} = \dot{u}^n + \Delta t\;\ddot{u}^{n+\gamma}. \tag{4.9}$$

At each time step, the problem (4.6)–(4.9) is equivalent to a linear complementarity problem and is well-posed. In contrast to the static case, the matrix K does not need to be positive definite for the problem to be well-posed (Dirichlet boundary conditions are not needed). When this scheme is tested on the first benchmark, we observe large spurious oscillations on the contact pressure and small spurious oscillations on the displacement during the contact phase (Figure 5). On the second benchmark, we observe a poor displacement and a poor energy behavior (Figure 6). Let us try to explain what happens exactly. Suppose that there is contact at the ith

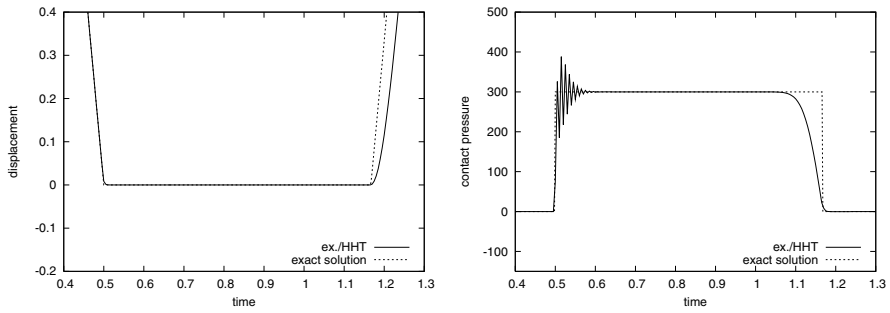

FIG. 7. *Impact of an elastic bar. Displacement u_0^n (left) and contact pressure r^n (right). Discretization* 4.1 *with* $\alpha = -0.2$, $\beta = 1/4(1-\alpha)^2$, $\gamma = 1/2 - \alpha$. $\Delta x = 0.1$, $\Delta t = 0.005$, $\nu_c = 1.5$.

node of the contact boundary at time t^{n+1} (i.e., $G_i u^{n+1} = 0$); then

$$G_i \dot{u}^{n+1} = -\frac{\gamma}{\beta \Delta t} G_i u^n + \left(1 - \frac{\gamma}{\beta}\right) G_i \dot{u}^n + \Delta t \frac{2\beta - \gamma}{2\beta} G_i \ddot{u}^n, \tag{4.10}$$

$$G_i \ddot{u}^{n+1} = -\frac{1}{\beta \Delta t^2} G_i u^n - \frac{1}{\beta \Delta t} G_i \dot{u}^n - \frac{1 - 2\beta}{2\beta} G_i \ddot{u}^n. \tag{4.11}$$

Thus, the impact law is not satisfied since we expect that after an impact, $G_i \dot{u}^{n+1} = G_i \ddot{u}^{n+1} = 0$. During a contact phase following an impact, the velocity and the acceleration oscillate. In the simple case of an impact without initial acceleration and initial velocity v_i, the magnitude of the acceleration oscillations after the impact is $\frac{v_i}{\Delta t}$. These oscillations trigger oscillations of magnitude $\frac{m_i v_i}{\Delta t}$ on the contact pressure, where m_i is the mass associated with the node i (Figure 5). Moreover, the energy balance takes the form

$$\mathcal{E}^{n+1} - \mathcal{E}^n = {}^{\mathrm{T}}\left(\frac{r^{n+1} + r^n}{2}\right)(Gu^{n+1} - Gu^n) + {}^{\mathrm{T}}\left(\frac{F^{n+1} + F^n}{2}\right)(u^{n+1} - u^n),$$

so that the contact force works when a node changes status. When a node comes into contact ($G_i u^n > 0$, $r^n = 0$, $G_i u^{n+1} = 0$, $r^{n+1} > 0$), the work is negative; when a node is released ($G_i u^n = 0$, $r^n > 0$, $G_i u^{n+1} > 0$, $r^{n+1} = 0$), the work is positive. As the contact pressure is polluted by large oscillations, this strongly perturbs the rest of the structure (Figure 6). The poor behavior of the Newmark scheme can be summarized as follows: large oscillations of the acceleration at the contact boundary $\Rightarrow$ large oscillations of the contact pressure $\Rightarrow$ perturbation of the whole structure.

In themselves the oscillations of the acceleration at the contact boundary are not a problem. The oscillations of the contact pressure are more troublesome if a Lagrangian method is used for solving the linear complementarity problem at each time step (the Lagrange multiplier being equal to the contact pressure). Of course, the perturbation of the whole structure must be avoided. Several options can be considered in designing better algorithms. The first option consists of using dissipative schemes, such as HHT schemes (Discretization 4.1). The spurious oscillations are then damped (Figure 7), but at the expense of poor energy behavior (Figure 8). The selected value $\alpha = -0.2$ here achieves a reasonable compromise between dissipation of spurious oscillations and energy. First-order schemes like θ-schemes, which are implicit, unconditionally stable, dissipative schemes, yield the same kind of results (Discretization 4.2).

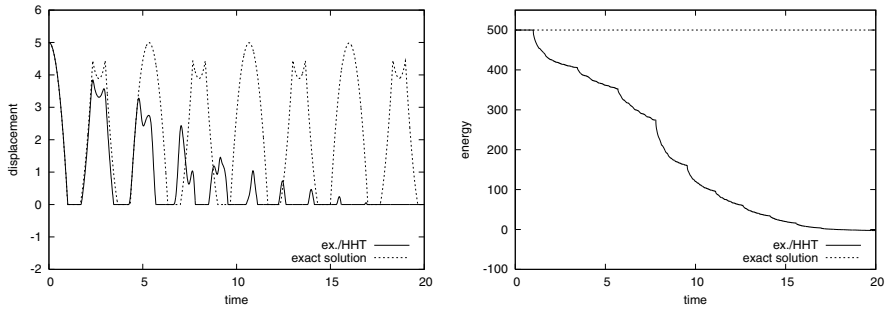

FIG. 8. *Bounces of an elastic bar. Displacement* u_0^n *(left) and energy* $\mathcal{E}^n - {}^{\mathrm{T}}Fu^n$ *(right). Discretization* 4.1 *with* $\alpha = -0.2$, $\beta = 1/4(1-\alpha)^2$, $\gamma = 1/2 - \alpha$. $\Delta x = 0.1$, $\Delta t = 0.005$, $\nu_c = 1.5$.

DISCRETIZATION 4.2 (θ-schemes [37]). *Seek* u^{n+1}, $\dot{u}^{n+1} \in \mathbb{R}^{N_d}$, *and* $r^{n+1} \in \mathbb{R}^{N_c}$ *such that*

$$M\ddot{u}^{n+\frac{1}{2}} + Ku^{n+\theta} = F^{n+\theta} + {}^{\mathrm{T}}Gr^{n+1}, \tag{4.12}$$

$$Gu^{n+1} \geq 0, \quad r^{n+1} \geq 0, \quad {}^{\mathrm{T}}r^{n+1}Gu^{n+1} = 0, \tag{4.13}$$

$$u^{n+1} = u^n + \Delta t\ \dot{u}^{n+\theta}, \tag{4.14}$$

$$\dot{u}^{n+1} = \dot{u}^n + \Delta t\ \ddot{u}^{n+\frac{1}{2}}. \tag{4.15}$$

Remark 4.4. It is sometimes argued in the literature that first-order schemes must be preferred to second-order schemes for dynamic contact problems, due to the nonsmoothness of the solution. We must distinguish two issues: the treatment of the contact condition and the treatment of the shock waves induced by the contact. As discussed previously, a proper treatment of the contact condition is not related to the order of the scheme. As for the shock waves, they require a scheme with dissipation, and there exist second-order accurate schemes with dissipation, such as the HHT or Chung–Hulbert schemes. Note also that the amount of dissipation needed to treat the shock waves in the bulk is much smaller than that needed to dissipate the oscillations caused by the contact condition.

4.1.2. Schemes dealing with the impact. First we briefly discuss a naive stabilized Newmark scheme where an extra step is used to enforce the impact law (Discretization 4.3). Then, we consider two schemes with dissipative contact using a midpoint (Discretization 4.4) or a Newmark (Discretization 4.5) scheme. Finally, an improvement of these schemes based on the velocity-update method introduced in [27] can be considered; in the case of the Newmark scheme, this yields Discretization 4.6. An alternative approach to prevent the oscillations of the acceleration from transferring to the contact pressure consists in removing the mass at the contact boundary. This approach will be developed in section 7.

To motivate the discussion, let us look for a scheme which satisfies the impact law or, more precisely, a scheme which forces the acceleration to be zero during the contact phases. No implicit Newmark scheme achieves this. An extra step is needed to enforce the impact law (Discretization 4.3).

DISCRETIZATION 4.3 (naive stabilized Newmark).

1. *Seek* $u^{n+1} \in \mathbb{R}^{N_d}$, $\dot{u}^{n+1} \in \mathbb{R}^{N_d}$, $\ddot{u}^{n+1} \in \mathbb{R}^{N_d}$, *and* $r^{n+1} \in \mathbb{R}^{N_c}$ *satisfying* (4.6)–(4.9).

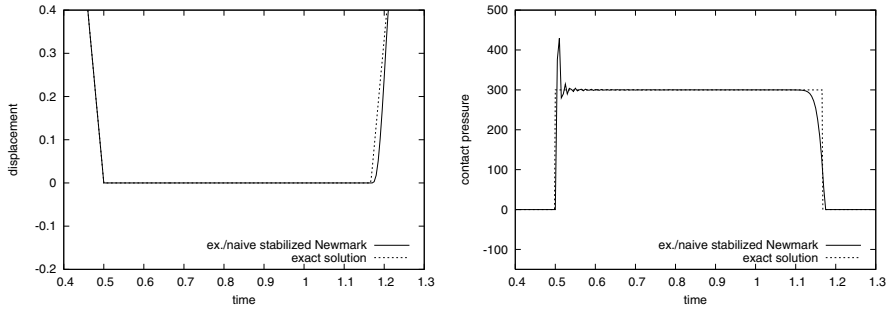

FIG. 9. *Impact of an elastic bar. Displacement* u_0^n *(left) and contact pressure* r^n *(right). Discretization* 4.3 *with* $\alpha = 0$, $\beta = 1/4$, *and* $\gamma = 1/2$. $\Delta x = 0.1$, $\Delta t = 0.005$, $\nu_c = 1.5$.

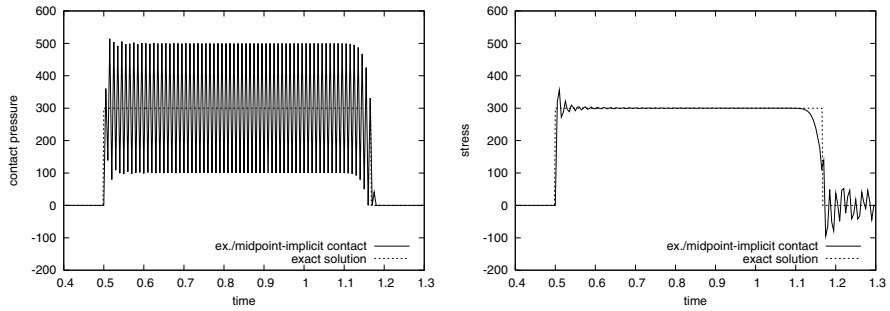

FIG. 10. *Impact of an elastic bar. Contact pressure* r^n *(left) and stress* $(Ku^n)_0$ *(right). Discretization* 4.4. $\Delta x = 0.1$, $\Delta t = 0.005$, $\nu_c = 1.5$.

2. *If* $G_i u^n \geq 0$ *and* $G_i u^{n+1} = 0$, *then* $\dot{u}^{n+1}$ *and* $\ddot{u}^{n+1}$ *are modified so that* $G_i \dot{u}^{n+1} = 0$ *and* $G_i \ddot{u}^{n+1} = 0$.

As illustrated in Figure 9, the large spurious oscillations have disappeared. However, this stabilization takes effect only one step after the impact, which explains the peak in the contact pressure just after the impact. A possible remedy consists of finding a time discretization where the contact force does not work or is at least dissipative. For instance, the midpoint scheme with an enforcement of the contact condition at time t^{n+1} (Discretization 4.4) achieves the following energy balance:

$$\mathcal{E}^{n+1} - \mathcal{E}^n = {}^{\mathrm{T}}r^{n+1}(Gu^{n+1} - Gu^n) + {}^{\mathrm{T}}F^{n+\frac{1}{2}}(u^{n+1} - u^n).$$

It is easy to check that the work of the contact force is always nonpositive. As illustrated in Figure 10, the contact pressure still oscillates, but the stress is practically free of oscillations. The oscillations of the stress after the bar has taken off are due to vibrations. However, energy losses, even if they are not substantial, do have an impact on the solution (Figure 11). It can also be noticed that energy losses do not vanish as Δt approaches zero, but these losses decrease with the mesh size.

DISCRETIZATION 4.4 (midpoint-implicit contact). *Seek* u^{n+1}, $\dot{u}^{n+1} \in \mathbb{R}^{N_d}$, *and* $r^{n+1} \in \mathbb{R}^{N_c}$ *such that*

$$M\ddot{u}^{n+\frac{1}{2}} + Ku^{n+\frac{1}{2}} = F^{n+\frac{1}{2}} + {}^{\mathrm{T}}Gr^{n+1}, \tag{4.16}$$

$$Gu^{n+1} \geq 0, \quad r^{n+1} \geq 0, \quad {}^{\mathrm{T}}r^{n+1}Gu^{n+1} = 0, \tag{4.17}$$

$$u^{n+1} = u^n + \Delta t\ \dot{u}^{n+\frac{1}{2}}, \tag{4.18}$$

$$\dot{u}^{n+1} = \dot{u}^n + \Delta t\ \ddot{u}^{n+\frac{1}{2}}. \tag{4.19}$$

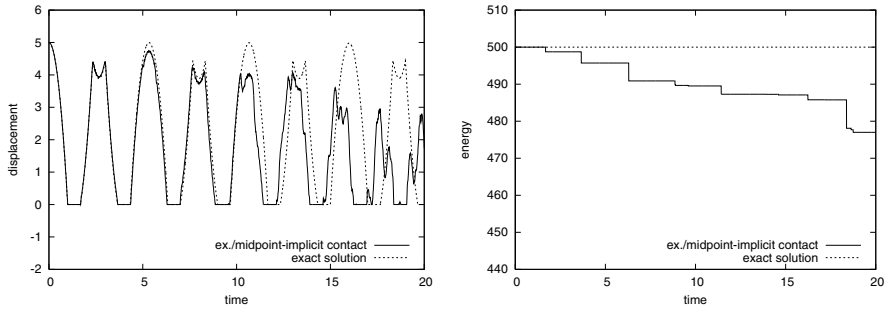

FIG. 11. *Bounces of an elastic bar. Displacement* u_0^n *(left) and energy* $\mathcal{E}^n - {}^{\mathrm{T}}Fu^n$ *(right). Discretization* 4.4. $\Delta x = 0.1$, $\Delta t = 0.005$, $\nu_c = 1.5$.

Another scheme with dissipative contact has been proposed in [18]. The Newmark scheme with parameters $\beta = 1/2$ and $\gamma = 1$ and with an enforcement of the contact condition at time t^{n+1} yields the following energy balance:

$$\mathcal{E}^{n+1} - \mathcal{E}^n = {}^{\mathrm{T}}r^{n+1}(Gu^{n+1} - Gu^n) - \frac{1}{2}{}^{\mathrm{T}}(u^{n+1} - u^n)K(u^{n+1} - u^n) + {}^{\mathrm{T}}F^{n+1}(u^{n+1} - u^n).$$

The work of the contact force is always nonpositive, but there is a strong bulk dissipation. To remove this dissipation, one can, as proposed in [18], discretize the acceleration coming from the contact forces with the dissipative parameters ($\beta = 1/2$ and $\gamma = 1$), and the acceleration coming from the elastic forces with a trapezoidal rule ($\beta = 1/4$ and $\gamma = 1/2$). This yields Discretization 4.5. With such a discretization, the energy balance is

$$\mathcal{E}^{n+1} - \mathcal{E}^n = {}^{\mathrm{T}}r^{n+1}(Gu^{n+1} - Gu^n) + {}^{\mathrm{T}}F^{n+1}(u^{n+1} - u^n).$$

The numerical results are similar to those obtained with Discretization 4.4.

DISCRETIZATION 4.5 (Newmark with dissipative contact [18]). *Seek* u^{n+1}, $\dot{u}^{n+1}$, $\ddot{u}_{int}^{n+1}$, $\ddot{u}_{con}^{n+1} \in \mathbb{R}^{N_d}$, *and* $r^{n+1} \in \mathbb{R}^{N_c}$ *such that*

$$M\ddot{u}^{n+1} + Ku^{n+1} = F^{n+1} + {}^{\mathrm{T}}Gr^{n+1}, \tag{4.20}$$

$$Gu^{n+1} \geq 0, \quad r^{n+1} \geq 0, \quad {}^{\mathrm{T}}r^{n+1}Gu^{n+1} = 0, \tag{4.21}$$

$$u^{n+1} = u^n + \Delta t\dot{u}^n + \frac{\Delta t^2}{2}\ddot{u}_{int}^{n+2\beta} + \frac{\Delta t^2}{2}\ddot{u}_{con}^{n+1}, \tag{4.22}$$

$$\dot{u}^{n+1} = \dot{u}^n + \Delta t\ddot{u}_{int}^{n+\gamma} + \Delta t\ddot{u}_{con}^{n+1}, \tag{4.23}$$

where $\ddot{u}^{n+1} = \ddot{u}_{int}^{n+1} + \ddot{u}_{con}^{n+1}$ *and* $M\ddot{u}_{con}^{n+1} = {}^{\mathrm{T}}Gr^{n+1}$.

To compensate for energy losses in schemes with dissipative contact, the so-called velocity-update method can be considered [27]. Applied to Discretization 4.4, this procedure does not significantly improve the solution on our second benchmark. In [8], the authors add to Discretization 4.5 a stabilization procedure (Discretization 4.6); for a consistency result under the assumption of viscoelastic material, see [22].

DISCRETIZATION 4.6 (stabilized Newmark [8]).

1. *Seek* $u_{pred}^{n+1} \in \mathbb{R}^{N_d}$ *and* $\lambda^{n+1} \in \mathbb{R}^{N_c}$ *such that*

$$Mu_{pred}^{n+1} = Mu^n + \Delta tM\dot{u}^n, \tag{4.24}$$

$$Gu_{pred}^{n+1} \geq 0, \quad \lambda^{n+1} \geq 0, \quad {}^{\mathrm{T}}\lambda^{n+1}Gu_{pred}^{n+1} = 0. \tag{4.25}$$

2. *Seek* $u^{n+1}, \dot{u}^{n+1}, \ddot{u}_{int}^{n+1},\ \ddot{u}_{con}^{n+1} \in \mathbb{R}^{N_d}$, *and* $r^{n+1} \in \mathbb{R}^{N_c}$ *satisfying* (4.20), (4.21), *and* (4.23), *while* (4.22) *is replaced by*

$$u^{n+1} = u_{pred}^{n+1} + \frac{\Delta t^2}{2}\ddot{u}_{int}^{n+2\beta} + \frac{\Delta t^2}{2}\ddot{u}_{con}^{n+1}. \tag{4.26}$$

The additional step required by Discretization 4.6 is not expensive compared with the main step, especially if the mass matrix is lumped. With this scheme, the contact pressure is now almost free of oscillations (Figure 12). Although the impact law is not fulfilled, $G_i\ddot{u}_{int}^{n+2\beta} + G_i\ddot{u}_{con}^{n+1} = 0$ holds true if $G_i u^{n+1} = G_i u_{pred}^{n+1} = 0$. Energy losses still remain sizeable in the second benchmark (Figure 13).

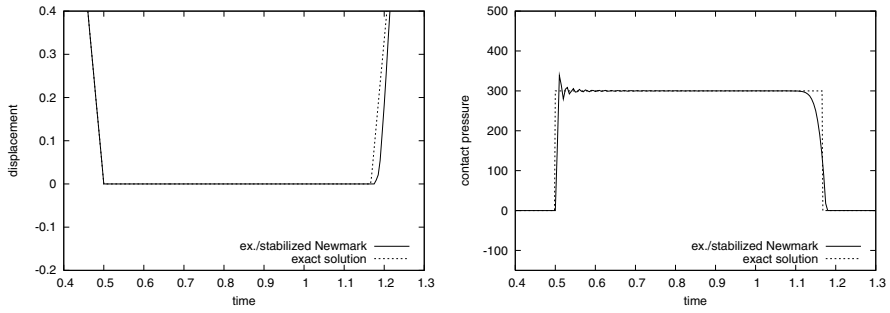

FIG. 12. *Impact of an elastic bar. Displacement* u_0^n *(left) and contact pressure* r^n *(right). Discretization* 4.6 *with* $\beta = 1/4$ *and* $\gamma = 1/2$ *(lumped mass matrix).* $\Delta x = 0.1$, $\Delta t = 0.005$, $\nu_c = 1.5$.

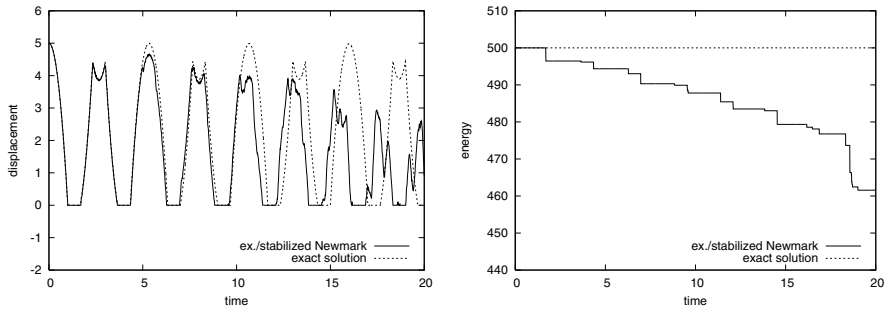

FIG. 13. *Bounces of an elastic bar. Displacement* u_0^n *(left) and energy* $\mathcal{E}^n - {}^{\mathrm{T}}Fu^n$ *(right). Discretization* 4.6 *with* $\beta = 1/4$ *and* $\gamma = 1/2$ *(lumped mass matrix).* $\Delta x = 0.1$, $\Delta t = 0.005$, $\nu_c = 1.5$.

4.2. Semiexplicit schemes. Now, we try to discretize the elastodynamics part of the problem with an explicit scheme, such as the central difference scheme. It is not possible to enforce an explicit exact contact condition. Nevertheless, the contact condition can be enforced implicitly as in [31, 32].

DISCRETIZATION 4.7 (central differences-implicit contact [31, 32]). *Seek* $u^{n+1} \in \mathbb{R}^{N_d}$ *and* $r^{n+1} \in \mathbb{R}^{N_c}$ *such that*

$$M\left(\frac{u^{n+1} - 2u^n + u^{n-1}}{\Delta t^2}\right) + Ku^n = F^n + {}^{\mathrm{T}}Gr^{n+1}, \tag{4.27}$$

$$Gu^{n+1} \geq 0, \quad r^{n+1} \geq 0, \quad {}^{\mathrm{T}}r^{n+1}Gu^{n+1} = 0. \tag{4.28}$$

With a lumped mass matrix, this scheme is equivalent to that proposed in [6] where the contact condition is enforced by a projection step in the following semiexplicit way (observe that the first step is explicit):

1. Seek $u^{n+1} \in \mathbb{R}^{N_d}$ such that

$$M\left(\frac{u^{n+1}-2u^n+u^{n-1}}{\Delta t^2}\right)+Ku^n=F^n. \tag{4.29}$$

2. If $G_i u^{n+1}<0$, then u^{n+1} is modified so that $G_i u^{n+1}=0$.

It is easy to check that, with Discretization 4.7, the acceleration at the contact boundary vanishes during a contact phase (after two steps). Indeed, if $G_i u^{n+1}=G_i u^n=G_i u^{n-1}=0$, then $G_i \ddot{u}^n = G_i\big(\frac{u^{n+1}-2u^n+u^{n-1}}{\Delta t^2}\big)=0$. Consequently, there are (almost) no spurious oscillations (Figure 14). The shifted energy balance reads

$$\mathcal{E}^{n+1}_{0,\frac{1}{2}}-\mathcal{E}^{n}_{0,\frac{1}{2}}={}^{\mathrm{T}}\left(\frac{r^{n+2}+r^{n+1}}{2}\right)(Gu^{n+1}-Gu^n)+{}^{\mathrm{T}}\left(\frac{F^{n+1}+F^n}{2}\right)(u^{n+1}-u^n).$$

Energy losses, although moderate, affect the quality of the solution after some impacts (Figure 15). In one dimension, the convergence of the discrete solutions to the continuous solution, provided a stability condition is met (the same as in the linear case), has been established in [34]. The convergence of the discrete solutions to a semidiscrete solution has been proven in [31, 32].

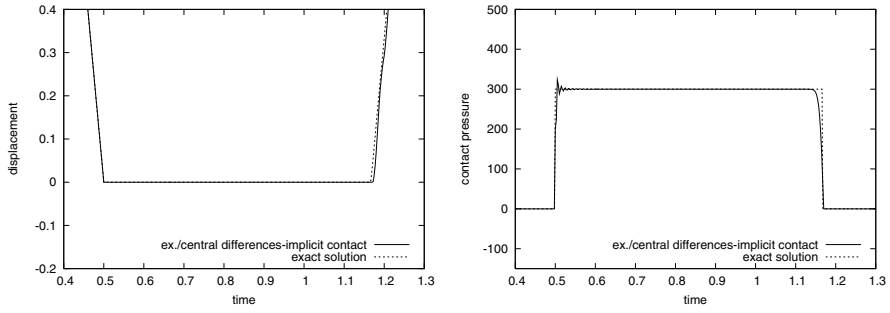

FIG. 14. *Impact of an elastic bar. Displacement u_0^n (left) and contact pressure r^n (right). Discretization* 4.7 *(lumped mass matrix).* $\Delta x=0.1$, $\Delta t=0.0025$, $\nu_c=0.75$.

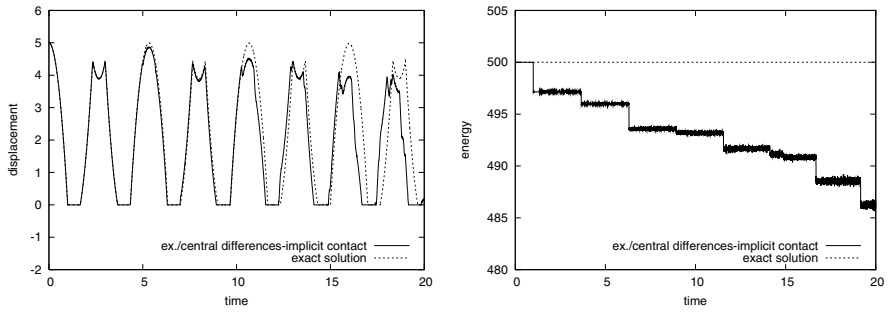

FIG. 15. *Bounces of an elastic bar. Displacement u_0^n (left) and energy $\mathcal{E}^n-{}^{\mathrm{T}}Fu^n$ (right). Discretization* 4.7 *(lumped mass matrix).* $\Delta x=0.1$, $\Delta t=0.0025$, $\nu_c=0.75$.

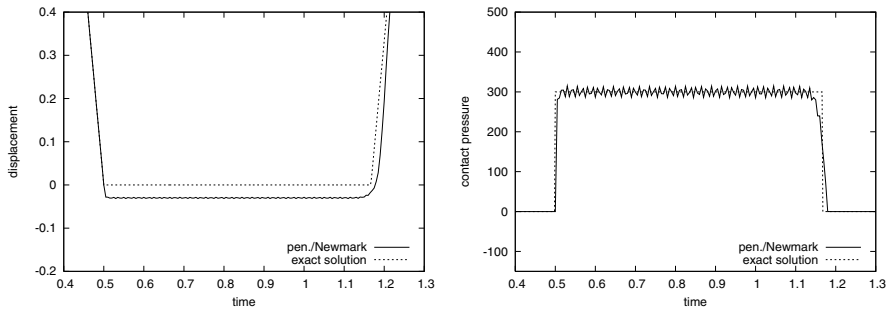

FIG. 16. *Impact of an elastic bar. Displacement* u_0^n *(left) and contact pressure* ${}^{\mathrm{T}}GR_\epsilon(Gu^n)$ *(right). Discretization* 5.1 *with* $\alpha = 0$, $\beta = 1/4$, $\gamma = 1/2$, $\epsilon = 10^{-4}$. $\Delta x = 0.1$, $\Delta t = 0.005$, $\nu_c = 1.5$.

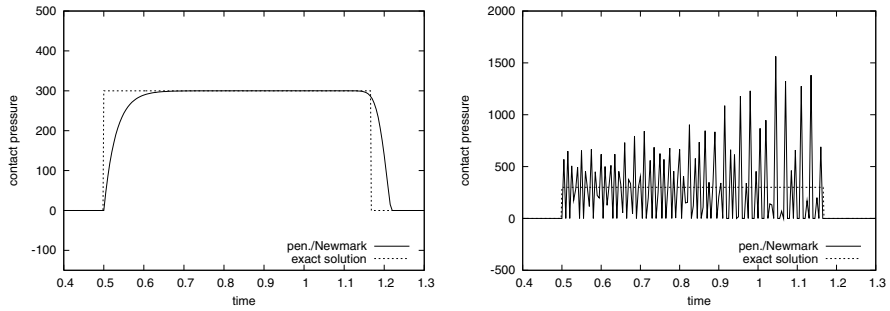

FIG. 17. *Impact of an elastic bar. Contact pressure* ${}^{\mathrm{T}}GR_\epsilon(Gu^n)$. *Discretization* 5.1 *with* $\alpha = 0$, $\beta = 1/4$, *and* $\gamma = 1/2$. $\Delta x = 0.1$, $\Delta t = 0.005$, $\nu_c = 1.5$. $\epsilon = 10^{-3}$ *(left) and* $\epsilon = 10^{-5}$ *(right).*

5. Discretizations with penalty contact condition. In this part we combine standard finite elements in space and a penalty approximation of the contact condition (the penalty parameter is denoted by ϵ). Then, the semidiscrete problem is a mere system of ODEs.

PROBLEM 5.1. *Seek a displacement* $u : [0,T] \to \mathbb{R}^{N_d}$ *such that, for all* $t \in [0,T]$,

$$M\ddot{u}(t) + Ku(t) = f(t) + {}^{\mathrm{T}}GR_\epsilon(Gu(t)), \tag{5.1}$$

with the initial conditions $u(0) = u^0$ *and* $\dot{u}(0) = v^0$.

Problem 5.1, being a system of ODEs with a Lipschitz continuous right-hand side, has one and only one solution, which is furthermore twice differentiable in time.

5.1. Implicit schemes. To begin with, we discretize Problem 5.1 with an implicit Newmark scheme.

DISCRETIZATION 5.1 (Newmark). *Seek* u^{n+1}, $\dot{u}^{n+1}$, $\ddot{u}^{n+1} \in \mathbb{R}^{N_d}$, *such that*

$$M\ddot{u}^{n+1} + Ku^{n+1} = F^{n+1} + {}^{\mathrm{T}}GR_\epsilon(Gu^{n+1}), \tag{5.2}$$

$$u^{n+1} = u^n + \Delta t\dot{u}^n + \frac{\Delta t^2}{2}\ddot{u}^{n+2\beta}, \tag{5.3}$$

$$\dot{u}^{n+1} = \dot{u}^n + \Delta t\ddot{u}^{n+\gamma}. \tag{5.4}$$

We observe that the penalty formulation tends to reduce spurious oscillations (Figure 16). Nevertheless, the oscillations grow with $1/\epsilon$ (Figure 17). This is not

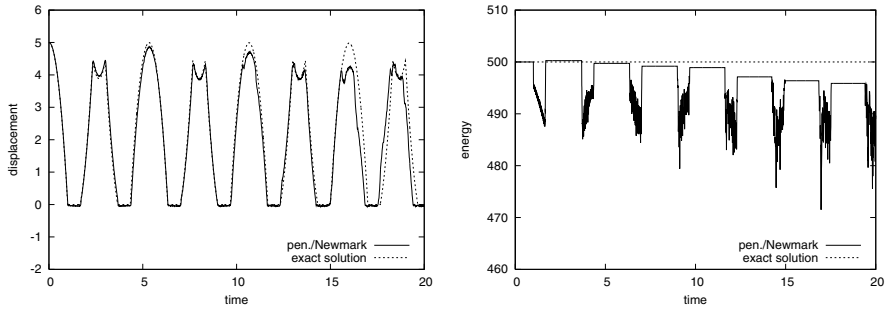

FIG. 18. *Bounces of an elastic bar. Displacement u_0^n (left) and energy $\mathcal{E}^n - {}^{\mathrm{T}}Fu^n$ (right). Discretization* 5.1 *with $\alpha = 0$, $\beta = 1/4$, $\gamma = 1/2$, and $\epsilon = 10^{-4}$. $\Delta x = 0.1$, $\Delta t = 0.005$, $\nu_c = 1.5$.*

surprising, since the penalty contact condition tends to the exact contact condition when $1/\epsilon$ tends to infinity. If the oscillations are too large, stabilization procedures can be used (see, for instance, the procedure described in [1]). With the addition of a penalty term, the Newmark scheme (trapezoidal rule) no longer conserves the energy. The energy losses are moderate but not so marginal (Figure 18); the energy behavior is poorer when $1/\epsilon$ grows. In [1, 15], the authors proposed a discretization of the penalty term which enables one to recover energy control by conserving an augmented energy (Discretization 5.2). It is based on a midpoint scheme. On our benchmark problems, it does not yield significantly better results.

DISCRETIZATION 5.2 (energy-controlling midpoint [1, 15]). *Seek u^{n+1}, $\dot{u}^{n+1} \in \mathbb{R}^{N_d}$ such that*

$$M\ddot{u}^{n+\frac{1}{2}} + Ku^{n+\frac{1}{2}} = F^{n+\frac{1}{2}} + {}^{\mathrm{T}}G\tilde{R}_\epsilon(Gu^{n+1}, Gu^n), \tag{5.5}$$

$$u^{n+1} = u^n + \Delta t\dot{u}^{n+\frac{1}{2}}, \tag{5.6}$$

$$\dot{u}^{n+1} = \dot{u}^n + \Delta t\ddot{u}^{n+\frac{1}{2}}, \tag{5.7}$$

where

$$(\tilde{R}_\epsilon(Gu^{n+1}, Gu^n))_i = \begin{cases} \frac{1}{2\epsilon}\frac{((G_iu^{n+1})^-)^2 - ((G_iu^n)^-)^2}{G_iu^{n+1} - G_iu^n} & \text{if } G_iu^n \neq G_iu^{n+1}, \\ 0 & \text{if } G_iu^n = G_iu^{n+1} \geq 0, \\ \frac{1}{2\epsilon}(Gu^{n+1} + Gu^n) & \text{if } G_iu^n = G_iu^{n+1} < 0. \end{cases} \tag{5.8}$$

Defining the augmented energy $\mathcal{E}^n_{pen} := \mathcal{E}^n + \frac{1}{2\epsilon}((Gu^n)^-)^2$, there holds

$$\mathcal{E}^{n+1}_{pen} - \mathcal{E}^n_{pen} = {}^{\mathrm{T}}F^{n+\frac{1}{2}}(u^{n+1} - u^n).$$

Since $\mathcal{E}^n_{pen}$ is an upper bound of $\mathcal{E}^n$, controlling $\mathcal{E}^n_{pen}$ allows one to control $\mathcal{E}^n$.

5.2. Explicit schemes. We can also use an explicit scheme for Problem 5.1.

DISCRETIZATION 5.3 (central differences). *Seek $u^{n+1} \in \mathbb{R}^{N_d}$ such that*

$$M\left(\frac{u^{n+1} - 2u^n + u^{n-1}}{\Delta t^2}\right) + Ku^n = F^n + {}^{\mathrm{T}}GR_\epsilon(Gu^n). \tag{5.9}$$

The results are similar to those obtained with the implicit approach. Unfortunately, the penalty term stiffens the system of ODEs, which limits the stability domain of the schemes. More precisely, it introduces a constraint on the time step of the form $\Delta t \leq O(\sqrt{\rho\epsilon\Delta x_c})$, where Δx_c is the mesh size near the contact boundary [3].

6. Discretizations with contact condition in velocity. In this section, standard finite elements in space are combined with an approximation of the contact condition involving the velocity.

PROBLEM 6.1. *Seek a displacement* $u : [0,T] \to \mathbb{R}^{N_d}$ *and a contact pressure* $r : [0,T] \to \mathbb{R}^{N_c}$ *such that, for almost every* $t \in [0,T]$,

$$M\ddot{u}(t) + Ku(t) = f(t) + {}^{\mathrm{T}}Gr(t), \tag{6.1}$$

$$G\dot{u}(t) \geq 0, \quad r(t) \geq 0, \quad {}^{\mathrm{T}}r(t)G\dot{u}(t) = 0, \tag{6.2}$$

with the initial conditions $u(0) = u^0$ *and* $\dot{u}(0) = v^0$.

With this contact condition in velocity, the semidiscrete problem is much simpler than (4.1)–(4.2). Problem 6.1 is still a system of ODEs under unilateral constraints, but the constraint now involves the velocity instead of the displacement. The general theory developed in [4, 12] applies to Problem 6.1. The solution u is unique [4]. Furthermore, u is continuous and $\dot{u}$ is differentiable in time almost everywhere, so that the equations have a sense at almost every time. The time discretization has been extensively studied in [12].

Unfortunately, the contact condition in velocity is not equivalent to the Signorini condition as discussed in section 2.3. The strategy adopted is the following: if a node satisfies the noninterpenetration condition, then at the next iteration no constraint is enforced on this node; if a node breaks the noninterpenetration condition, then at the next iteration the contact condition in velocity will be applied to this node. This approach allows for slight interpenetration. At each time step, we define the matrix G^n whose rows G_i^n are

$$G_i^n = \begin{cases} (0 \dots 0) & \text{if } G_i u^n \geq 0, \\ G_i & \text{if } G_i u^n < 0. \end{cases} \tag{6.3}$$

This approach based on a contact condition in velocity has also been widely used in rigid-body dynamics with impacts (see, e.g., [35]).

6.1. Implicit schemes. A midpoint scheme with contact condition in velocity has been proposed in [26]; see also [19] for the contact condition.

DISCRETIZATION 6.1 (midpoint [26]). *Seek* u^{n+1}, $\dot{u}^{n+1} \in \mathbb{R}^{N_d}$, *and* $r^{n+1} \in \mathbb{R}^{N_c}$ *such that*

$$M\ddot{u}^{n+\frac{1}{2}} + Ku^{n+\frac{1}{2}} = F^{n+\frac{1}{2}} + {}^{\mathrm{T}}G^n r^{n+\frac{1}{2}}, \tag{6.4}$$

$$G^n \dot{u}^{n+\frac{1}{2}} \geq 0, \quad r^{n+\frac{1}{2}} \geq 0, \quad {}^{\mathrm{T}}r^{n+\frac{1}{2}} G^n \dot{u}^{n+\frac{1}{2}} = 0, \tag{6.5}$$

$$u^{n+1} = u^n + \Delta t\ \dot{u}^{n+\frac{1}{2}}, \tag{6.6}$$

$$\dot{u}^{n+1} = \dot{u}^n + \Delta t\ \ddot{u}^{n+\frac{1}{2}}. \tag{6.7}$$

An interesting feature of this scheme is to be energy-conserving,

$$\mathcal{E}^{n+1} - \mathcal{E}^n = {}^{\mathrm{T}}F^{n+\frac{1}{2}}(u^{n+1} - u^n).$$

The contact pressure does not perturb the structure despite its oscillations (Figure 19). Energy is preserved, and the solution for the second benchmark is quite satisfactory, although not as accurate as with Discretization 5.1 after several impacts (Figure 20).

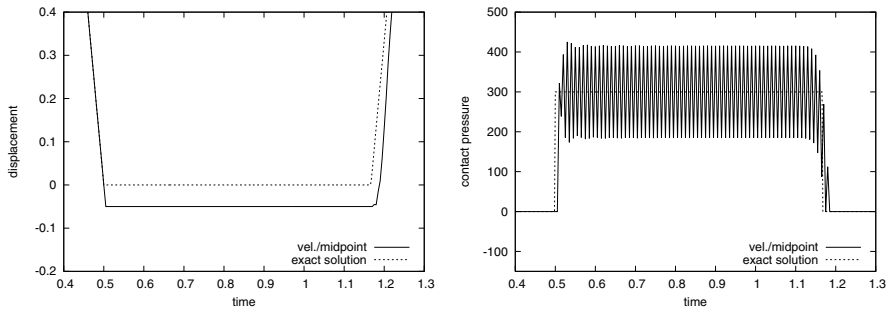

FIG. 19. *Impact of an elastic bar. Displacement u_0^n (left) and stress (right). Discretization* 6.1 *with $\alpha = 0$, $\beta = 1/4$, and $\gamma = 1/2$. $\Delta x = 0.1$, $\Delta t = 0.005$, $\nu_c = 1.5$.*

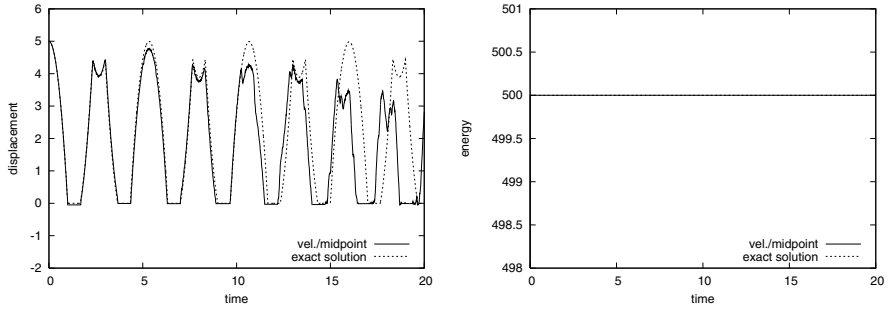

FIG. 20. *Bounces of an elastic bar. Displacement u_0^n (left) and energy $\mathcal{E}^n - {}^{\mathrm{T}}Fu^n$ (right). Discretization* 6.1 *with $\alpha = 0$, $\beta = 1/4$, and $\gamma = 1/2$. $\Delta x = 0.1$, $\Delta t = 0.005$, $\nu_c = 1.5$.*

6.2. Semiexplicit schemes. A semiexplicit scheme with contact condition in velocity has been proposed in [3].

DISCRETIZATION 6.2 (central differences [3]). *Seek $u^{n+1} \in \mathbb{R}^{N_d}$ and $r^{n+1} \in \mathbb{R}^{N_c}$ such that*

$$M\left(\frac{u^{n+1} - 2u^n + u^{n-1}}{\Delta t^2}\right) + Ku^n = F^n + {}^{\mathrm{T}}G^n r^{n+1}, \tag{6.8}$$

$$G^n(u^{n+1} - u^n) \geq 0, \quad r^{n+1} \geq 0, \quad {}^{\mathrm{T}}r^{n+1}G^n(u^{n+1} - u^n) = 0. \tag{6.9}$$

Numerical simulations suggest that the stability condition of the central difference scheme is not tightened by the contact condition. The results are similar to those obtained with Discretization 4.7 (Figures 21 and 22).

7. Discretizations with modified mass. In the previous three sections, we have considered various ways of enforcing the contact condition. Here we describe methods based on a modification of the mass matrix. Such methods are thus compatible with any enforcement of the contact condition. For brevity, we restrict ourselves to an exact enforcement of the contact condition. In the modified mass matrix, the entries associated with the normal displacements at the contact boundary are set to zero. The motivation for this modification is very simple: if the mass is removed, the inertial forces and the oscillations are eliminated. This approach was introduced in [20].

Set $N_d^* := N_d - N_c$. For the sake of simplicity, suppose that the degrees of freedom associated with normal displacements at the contact boundary are numbered

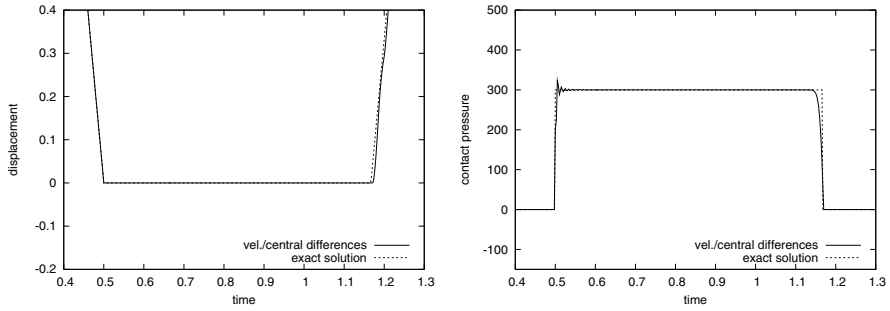

FIG. 21. *Impact of an elastic bar. Displacement* u_0^n *(left) and contact pressure* r^n *(right). Discretization* 6.2 *(lumped mass matrix).* $\Delta x = 0.1$, $\Delta t = 0.0025$, $\nu_c = 0.75$.

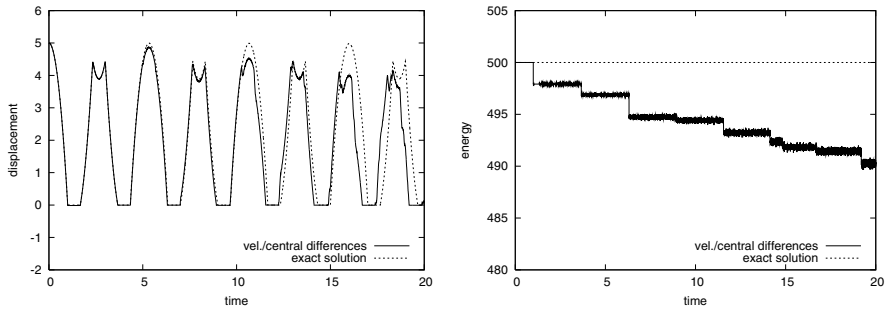

FIG. 22. *Bounces of an elastic bar. Displacement* u_0^n *(left) and energy* $\mathcal{E}^n - {}^{\mathrm{T}}Fu^n$ *(right). Discretization* 6.2 *(lumped mass matrix).* $\Delta x = 0.1$, $\Delta t = 0.0025$, $\nu_c = 0.75$.

from $N_d^* + 1$ to N_d. The modified mass matrix is defined as

$$M^* = \begin{pmatrix} M_{**} & 0 \\ 0 & 0 \end{pmatrix}.$$

Many choices are possible in building the block M_{**}. In [14, 20], the authors devise various methods for preserving some features of the standard mass matrix (the total mass, the center of gravity, and the moments of inertia); see also [33] for further results. We can also simply keep the corresponding block in the standard mass matrix (and this is what we will do in our numerical simulations below). The modified problem reads

$$M^*\ddot{u}(t) + Ku(t) = F(t) + {}^{\mathrm{T}}Gr(t), \tag{7.1}$$

$$Gu(t) \geq 0, \quad r(t) \geq 0, \quad {}^{\mathrm{T}}r(t)Gu(t) = 0. \tag{7.2}$$

If we set $u(t) = \begin{pmatrix} u_*(t) \\ u_c(t) \end{pmatrix}$, $K = \begin{pmatrix} K_{**} & K_{*c} \\ K_{c*} & K_{cc} \end{pmatrix}$, $F(t) = \begin{pmatrix} F_*(t) \\ F_c(t) \end{pmatrix}$, and $G = (0\ G_c)$, then (7.1) and (7.2) can be recast as

$$M_{**}\ddot{u}_*(t) + K_{**}u_*(t) + K_{*c}u_c(t) = F_*(t), \tag{7.3}$$

$$K_{c*}u_*(t) + K_{cc}u_c(t) = F_c(t) + {}^{\mathrm{T}}G_c r(t), \tag{7.4}$$

$$G_c u_c(t) \geq 0, \quad r(t) \geq 0, \quad {}^{\mathrm{T}}r(t)G_c u_c(t) = 0. \tag{7.5}$$

For given t and $u_*(t)$, there exists one and only one $u_c(t)$ satisfying (7.4) and (7.5). Denote by $Q : [0,T] \times \mathbb{R}^{N_d^*} \to \mathbb{R}^{N_c}$ the nonlinear map such that $u_c(t) = Q(t, u_*(t))$.

PROBLEM 7.1. *Seek a displacement $u : [0,T] \to \mathbb{R}^{N_d}$ such that, for all $t \in [0,T]$,*

$$M_{**}\ddot{u}_*(t) + K_{**}u_*(t) + K_{*c}Q(t, u_*(t)) = F_*(t), \tag{7.6}$$

$$u_c(t) = Q(t, u_*(t)), \tag{7.7}$$

with the initial conditions $u(0) = u^0$ and $\dot{u}(0) = v^0$.

The operator $Q(t,\cdot)$ is Lipschitz continuous at each time t, so that (7.6) is a Lipschitz system of ODEs. Therefore, it has a unique solution u_*, twice differentiable in time. Owing to (7.7), u_c is differentiable in time almost everywhere. The detailed mathematical analysis of the space semidiscrete modified mass formulation can be found in [20, 9]. A result of convergence of the space semidiscrete solutions to a continuous solution is proven for viscoelastic materials in [9].

Remark 7.1. In contrast to the semidiscrete problem with standard mass matrix, the semidiscrete problem with modified mass matrix does not require an impact law and conserves a modified energy where the mass modification is accounted for in the kinetic energy [20].

7.1. Implicit schemes. An HHT-Newmark scheme can be used for Problem 7.1.

DISCRETIZATION 7.1 (HHT-Newmark [20]). *Seek $u^{n+1} \in \mathbb{R}^{N_d}$, $\dot{u}_*^{n+1} \in \mathbb{R}^{N_d}$, and $\ddot{u}_*^{n+1} \in \mathbb{R}^{N_d}$ such that*

$$M_{**}\ddot{u}_*^{n+1} + K_{**}u_*^{n+1+\alpha} + K_{*c}Q(t^{n+1+\alpha}, u_*^{n+1+\alpha}) = F_*^{n+1+\alpha}, \tag{7.8}$$

$$u_c^{n+1+\alpha} = Q(t^{n+1+\alpha}, u_*^{n+1+\alpha}), \tag{7.9}$$

$$u_*^{n+1} = u_*^n + \Delta t\dot{u}_*^n + \frac{\Delta t^2}{2}\ddot{u}_*^{n+2\beta}, \tag{7.10}$$

$$\dot{u}_*^{n+1} = \dot{u}_*^n + \Delta t\ddot{u}_*^{n+\gamma}. \tag{7.11}$$

The equations can be recast as a linear complementarity problem,

$$M^*\ddot{u}^{n+1} + Ku^{n+1+\alpha} = F^{n+1+\alpha} + {}^{\mathrm{T}}Gr^{n+1}, \tag{7.12}$$

$$Gu^{n+1} \geq 0, \quad r^{n+1} \geq 0, \quad {}^{\mathrm{T}}r^{n+1}Gu^{n+1} = 0, \tag{7.13}$$

$$u^{n+1} = u^n + \Delta t\dot{u}^n + \frac{\Delta t^2}{2}\ddot{u}^{n+2\beta}, \tag{7.14}$$

$$\dot{u}^{n+1} = \dot{u}^n + \Delta t\ddot{u}^{n+\gamma}. \tag{7.15}$$

In spite of the modification of the mass matrix, the problem is well-posed. In practice, we use this set of equations to compute the solution. As expected, the large oscillations have disappeared during the contact phase (Figure 23). The energy behavior is also very satisfactory (Figure 24), since

$$\mathcal{E}_*^{n+1} - \mathcal{E}_*^n = {}^{\mathrm{T}}\left(\frac{r^{n+1}+r^n}{2}\right)(Gu^{n+1} - Gu^n) + {}^{\mathrm{T}}\left(\frac{F^{n+1}+F^n}{2}\right)(u^{n+1} - u^n),$$

where the modified energy $\mathcal{E}_*^n$ has the same expression as $\mathcal{E}^n$, except that M is replaced by M^*. The displacement after several impacts is quite satisfactory, although not as accurate as with Discretization 5.1 (Figure 24).

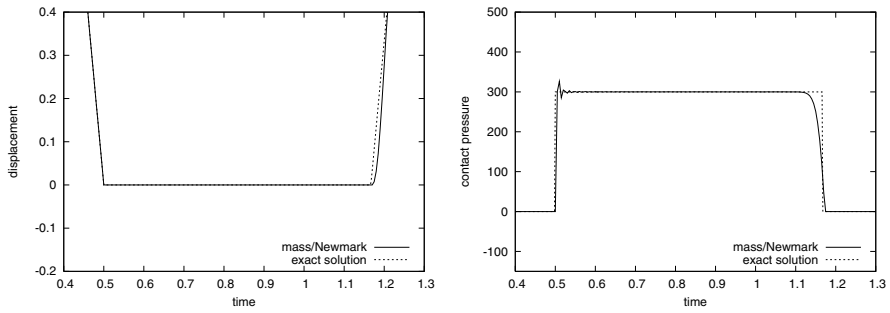

FIG. 23. *Impact of an elastic bar. Displacement* u_0^n *and contact pressure* r^n*. Discretization* 7.1 *with* $\alpha = 0$*,* $\beta = 1/4$*, and* $\gamma = 1/2$*.* $\Delta x = 0.1$*,* $\Delta t = 0.005$*,* $\nu_c = 1.5$*.*

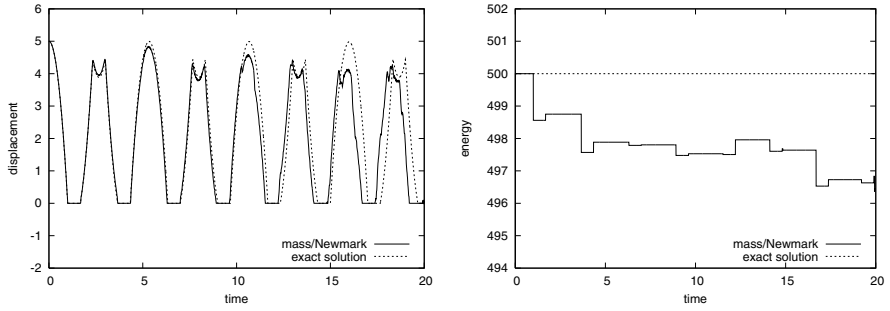

FIG. 24. *Bounces of an elastic bar. Displacement* u_0^n *(left) and modified energy* $\mathcal{E}_*^n - {}^{\mathrm{T}}Fu^n$ *(right). Discretization* 7.1 *with* $\alpha = 0$*,* $\beta = 1/4$*, and* $\gamma = 1/2$*.* $\Delta x = 0.1$*,* $\Delta t = 0.005$*,* $\nu_c = 1.5$*.*

7.2. Semiexplicit schemes. We can discretize Problem 7.1 with an explicit scheme, such as the central difference scheme. This yields a semiexplicit scheme.

DISCRETIZATION 7.2 (central differences [10]). *Seek* $u^{n+1} \in \mathbb{R}^{N_d}$ *such that*

$$M_{**}\left(\frac{u_*^{n+1} - 2u_*^n + u_*^{n-1}}{\Delta t^2}\right) + K_{**}u_*^n + K_{*c}Q(t^n, u_*^n) = F_*^n, \tag{7.16}$$

$$u_c^{n+1} = Q(t^{n+1}, u_*^{n+1}). \tag{7.17}$$

In practice, the equations are solved as follows: 1. Seek $u_*^{n+1} \in \mathbb{R}^{N_d}$ such that

$$M_{**}\left(\frac{u_*^{n+1} - 2u_*^n + u_*^{n-1}}{\Delta t^2}\right) + K_{**}u_*^n + K_{*c}u_c^n = F_*^n. \tag{7.18}$$

2. Seek $u_c^{n+1} \in \mathbb{R}^{N_d^*}$ and $r^{n+1} \in \mathbb{R}^{N_c}$ such that

$$K_{c*}u_*^{n+1} + K_{cc}u_c^{n+1} = F_c^{n+1} + {}^{\mathrm{T}}G_c r^{n+1}, \tag{7.19}$$

$$G_c u_c^{n+1} \geq 0, \quad r^{n+1} \geq 0, \quad {}^{\mathrm{T}}rG_c u_c^{n+1} = 0. \tag{7.20}$$

The first step is explicit, and the mass matrix M_{**} can be lumped. The second step is a constrained problem on the variable u_c^{n+1} only. Discretization 7.2 amounts to

$$M^*\left(\frac{u^{n+1} - 2u^n + u^{n-1}}{\Delta t^2}\right) + Ku^n = F^n + {}^{\mathrm{T}}Gr^n,$$
$$Gu^n \geq 0, \quad r^n \geq 0, \quad {}^{\mathrm{T}}r^n Gu^n = 0,$$

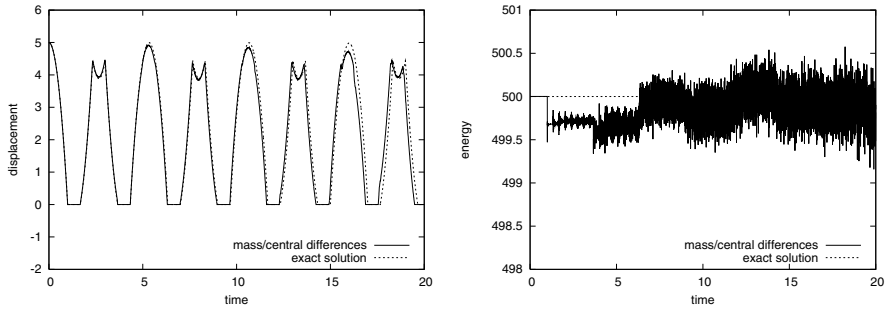

FIG. 25. *Bounces of an elastic bar. Displacement u_0^n (left) and modified energy $\mathcal{E}_*^n - {}^{\mathrm{T}}Fu^n$ (right). Discretization 7.2 (lumped mass matrix).* $\Delta x = 0.1$, $\Delta t = 0.0025$, $\nu_c = 0.75$.

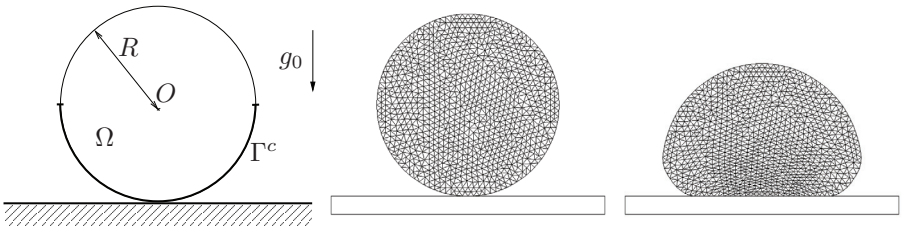

FIG. 26. *Bounces of an elastic disk. Reference configuration (left), mesh (middle), and deformed configuration after the first impact (right).*

and yields the modified shifted energy balance

$$\mathcal{E}^{n+1}_{0,\frac{1}{2}*} - \mathcal{E}^{n}_{0,\frac{1}{2}*} = {}^{\mathrm{T}}\left(\frac{r^{n+1}+r^n}{2}\right)(Gu^{n+1}-Gu^n) + {}^{\mathrm{T}}\left(\frac{F^{n+1}+F^n}{2}\right)(u^{n+1}-u^n),$$

where $\mathcal{E}^n_{0,\frac{1}{2}*}$ has the same expression than $\mathcal{E}^n_{0,\frac{1}{2}}$, except that M is replaced by M^*. We observe numerically that the stability condition on the time step is the same as in the linear case. Compared with Discretizations 4.7 and 6.2, the semiexplicit modified mass method shows a better energy behavior and a better solution (Figure 25). Additional tests show that the amplitude of energy oscillations decreases at least linearly with Δt at fixed Courant number. Results on the first benchmark are similar to those with the implicit scheme.

8. A 2D benchmark. We consider the bounces of an elastic disk against a rigid ground (Figure 26). The reference configuration is the undeformed disk touching the ground. The disk is dropped, undeformed, with a zero initial velocity, under a gravity acceleration g_0, the displacement of its center being initially h_0. The disk has radius R. The material is supposed to be linear elastic (plane strain) with a Young modulus E, a Poisson ratio ν, and a mass density ρ. The contact boundary Γ^c is the lower half of the disk boundary. We define the contact condition using the normal vector to the ground. The parameters are $E = 4000$, $\nu = 0.2$, $\rho = 100$, $g_0 = 5$, $R = 1$, $h_0 = 0.1$. The disk is meshed with triangles (100 edges on the boundary, 1804 triangles, 953 vertices; see Figure 26) and we use linear finite elements. The number of nodes lying on the contact boundary is 51. Simulations are performed using FREEFEM++ [16]. The Courant number is defined as $\nu_c := c_d \frac{\Delta x}{\Delta t}$, where $c_d = \frac{20}{3}$ is the speed of dilatational waves and $\Delta x = 0.0628$ the length of boundary edges.

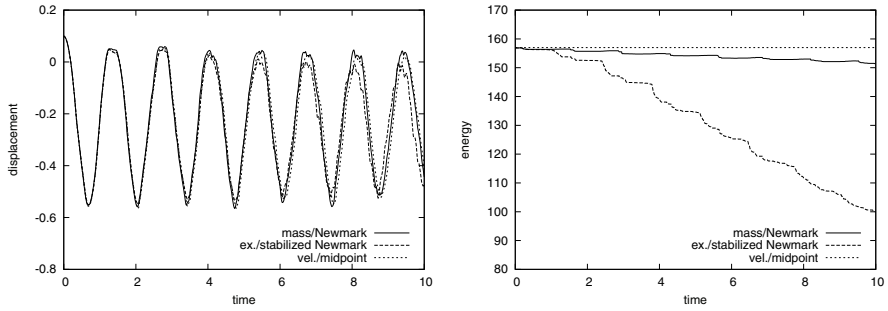

FIG. 27. *Bounces of an elastic disk. Displacement of its center (left) and energy or modified energy (right). Discretizations* 4.6, 6.1, *and* 7.1. $\Delta t = 0.01$, $\nu_c = 1.06$.

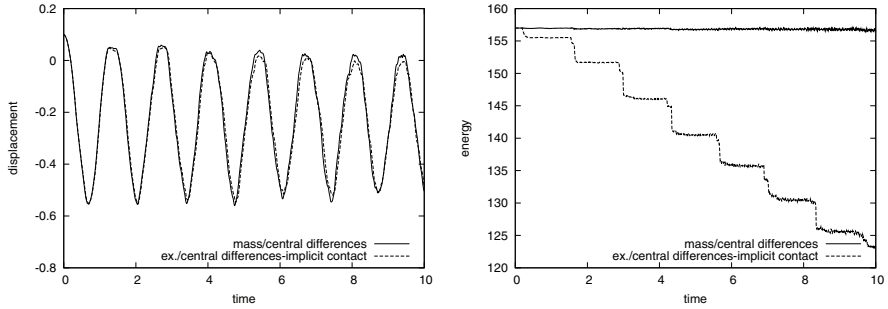

FIG. 28. *Bounces of an elastic disk. Displacement of its center (left) and energy or modified energy (right). Discretizations* 4.7 *and* 7.2. $\Delta t = 0.005$, $\nu_c = 0.53$.

Results are presented for the implicit Discretizations 4.6, 6.1, and 7.1 (Figure 27) and for the semiexplicit Discretizations 4.7 and 7.2 (Figure 28). For the semiexplicit schemes, the observed stability condition is $\nu_c \leq 0.65$. In all cases, the trajectory of the disk center is rather well captured, with some discrepancies appearing after five bounces. The energy behaviors remain consistent with those observed in one dimension. Note that the present choice of parameters is somewhat severe for energy behavior because of the relatively high impact velocity and low Young modulus.

9. Conclusions. In this work, we have reviewed various time-integration schemes for the finite element dynamic Signorini problem. We have classified the schemes into four groups, the first three depending on the way the contact condition is enforced while the fourth group corresponds to modifying the mass matrix at the contact boundary. We have tested in detail the various schemes on two 1D benchmarks, both with analytical solution. The second benchmark is new and allows one to study the energy behavior within multiple impacts. Some selected schemes with favorable properties have been further compared on a 2D benchmark. All in all, we believe that the schemes with modified mass matrix, either implicit or semiexplicit, offer attractive properties, including ease of implementation, robustness, and relatively firm mathematical ground. The semiexplicit scheme with modified mass is new and stems from the combination of two existing ideas. We hope that the present results will stimulate further interest in the analysis and testing of these schemes.

REFERENCES

[1] F. Armero and E. Petocz, *Formulation and analysis of conserving algorithms for frictionless dynamic contact/impact problems*, Comput. Methods Appl. Mech. Engrg., 158 (1998), pp. 269–300.

[2] Y. Ayyad, M. Barboteu, and J. Fernandez, *A frictionless viscoelastodynamic contact problem with energy consistent properties: Numerical analysis and computational aspects*, Comput. Methods Appl. Mech. Engrg., 198 (2009), pp. 669–679.

[3] T. Belytschko and M. Neal, *Contact-impact by the pinball algorithm with penalty and Lagrangian methods*, Internat. J. Numer. Methods Engrg., 31 (1991), pp. 547–572.

[4] H. Brézis and J.-L. Lions, *Sur certains problèmes unilatéraux hyperboliques*, C. R. Acad. Sci. Paris Sér. A, 264 (1967), pp. A928–A931.

[5] B. Brogliato, *Nonsmooth Impact Mechanics*, Springer-Verlag, London, 1996.

[6] N. Carpenter, R. Taylor, and M. Katona, *Lagrange constraints for transient finite element surface contact*, Internat. J. Numer. Methods Engrg., 32 (1991), pp. 103–128.

[7] R. Courant and D. Hilbert, *Methods of Mathematical Physics. Vol.* I, Interscience, New York, 1953.

[8] P. Deuflhard, R. Krause, and S. Ertel, *A contact-stabilized Newmark method for dynamical contact problems*, Internat. J. Numer. Methods Engrg., 73 (2008), pp. 1274–1290.

[9] D. Doyen and A. Ern, *Convergence of a space semi-discrete modified mass method for the dynamic Signorini problem*, Commun. Math. Sci., 7 (2009), pp. 1063–1072.

[10] D. Doyen, A. Ern, and S. Piperno, *A Semi-explicit Modified Mass Method for Dynamic Contact Problems*, Lectures Notes in Appl. Comput. Mech., Springer, New York, 2010.

[11] C. Eck, J. Jarusek, and M. Krbec, *Unilateral Contact Problems. Variational Methods and Existence Theorems*, Chapman & Hall/CRC, Boca Raton, FL, 2005.

[12] R. Glowinski, J.-L. Lions, and R. Trémolières, *Numerical Analysis of Variational Inequalities*, North–Holland, Amsterdam, 1981.

[13] E. Grosu and I. Harari, *Stability of semidiscrete formulations for elastodynamics at small time steps*, Finite Elem. Anal. Des., 43 (2007), pp. 533–542.

[14] C. Hager, S. Hüeber, and B. I. Wohlmuth, *A stable energy-conserving approach for frictional contact problems based on quadrature formulas*, Internat. J. Numer. Methods Engrg., 73 (2008), pp. 205–225.

[15] P. Hauret and P. Le Tallec, *Energy-controlling time integration methods for nonlinear elastodynamics and low-velocity impact*, Comput. Methods Appl. Mech. Engrg., 195 (2006), pp. 4890–4916.

[16] F. Hecht and O. Pironneau, *FreeFEM++*, software, available online from www.freefem.org.

[17] T. J. R. Hughes, *The Finite Element Method*, Prentice–Hall, Englewood Cliffs, NJ, 1987.

[18] C. Kane, E. A. Repetto, M. Ortiz, and J. E. Marsden, *Finite element analysis of nonsmooth contact*, Comput. Methods Appl. Mech. Engrg., 180 (1999), pp. 1–26.

[19] H. B. Khenous, P. Laborde, and Y. Renard, *Comparison of two approaches for the discretization of elastodynamic contact problems*, C. R. Math. Acad. Sci. Paris, 342 (2006), pp. 791–796.

[20] H. B. Khenous, P. Laborde, and Y. Renard, *Mass redistribution method for finite element contact problems in elastodynamics*, Eur. J. Mech. A Solids, 27 (2008), pp. 918–932.

[21] N. Kikuchi and J. T. Oden, *Contact Problems in Elasticity: A Study of Variational Inequalities and Finite Element Methods*, SIAM Stud. Appl. Math. 8, SIAM, Philadelphia, PA, 1988.

[22] C. Klapproth, A. Schiela, and P. Deuflhard, *Consistency results for the contact-stabilized Newmark method*, Numer. Math., 116 (2010), pp. 65–94.

[23] R. Krause and M. Walloth, *Presentation and Comparison of Selected Algorithms for Dynamic Contact Based on the Newmark Scheme*, technical report, Institute of Computational Science, Università della Svizzera italiana, 2009.

[24] S. Krenk, *Energy conservation in Newmark based time integration algorithms*, Comput. Methods Appl. Mech. Engrg., 195 (2006), pp. 6110–6124.

[25] T. A. Laursen, *Computational Contact and Impact Mechanics*, Springer-Verlag, Berlin, 2002.

[26] T. A. Laursen and V. Chawla, *Design of energy conserving algorithms for frictionless dynamic contact problems*, Internat. J. Numer. Methods Engrg., 40 (1997), pp. 863–886.

[27] T. A. Laursen and G. R. Love, *Improved implicit integrators for transient impact problems—Geometric admissibility within the conserving framework*, Internat. J. Numer. Methods Engrg., 53 (2002), pp. 245–274.

[28] G. Lebeau and M. Schatzman, *A wave problem in a half-space with a unilateral constraint at the boundary*, J. Differential Equations, 53 (1984), pp. 309–361.

[29] J. J. Moreau, *Numerical aspects of the sweeping process. Computational modeling of contact and friction*, Comput. Methods Appl. Mech. Engrg., 177 (1999), pp. 329–349.
[30] N. Nsiampa, J.-P. Ponthot, and L. Noels, *Comparative study of numerical explicit schemes for impact problems*, Internat. J. Impact Engrg., 35 (2008), pp. 1688–1694.
[31] L. Paoli and M. Schatzman, *A numerical scheme for impact problems.* I: *The one-dimensional case*, SIAM J. Numer. Anal., 40 (2002), pp. 702–733.
[32] L. Paoli and M. Schatzman, *A numerical scheme for impact problems.* II: *The multidimensional case*, SIAM J. Numer. Anal., 40 (2002), pp. 734–768.
[33] Y. Renard, *The singular dynamic method for constrained second order hyperbolic equations: Application to dynamic contact problems*, J. Comput. Appl. Math., 234 (2010), pp. 906–923.
[34] M. Schatzman and M. Bercovier, *Numerical approximation of a wave equation with unilateral constraints*, Math. Comp., 53 (1989), pp. 55–79.
[35] D. E. Stewart, *Rigid-body dynamics with friction and impact*, SIAM Rev., 42 (2000), pp. 3–39.
[36] R. Taylor and P. Papadopoulos, *On a finite element method for dynamic contact/impact problems*, Internat. J. Numer. Methods Engrg., 36 (1993), pp. 2123–2140.
[37] D. Vola, E. Pratt, M. Jean, and M. Raous, *Consistent time discretization for dynamical contact problems and complementarity techniques*, Rev. Europ. Elém. Finis, 7 (1998), pp. 149–162.
[38] P. Wriggers, *Computational Contact Mechanics*, John Wiley & Sons, New York, 2002.